In Press Physical Review A (2003)

Asymptotically Improved Convergence of Optimized Perturbation Theory in the Bose-Einstein Condensation Problem

Jean-Loïc Kneur,[1,*] Marcus B. Pinto,[1,2,†] and Rudnei O. Ramos[3,‡]

[1] *Laboratoire de Physique Mathématique et Théorique - CNRS - UMR 5825 Université Montpellier II, France*
[2] *Departamento de Física, Universidade Federal de Santa Catarina, 88040-900 Florianópolis, SC, Brazil*
[3] *Departamento de Física Teórica, Universidade do Estado do Rio de Janeiro, 20550-013 Rio de Janeiro, RJ, Brazil*

We investigate the convergence properties of optimized perturbation theory, or linear δ expansion (LDE), within the context of finite temperature phase transitions. Our results prove the reliability of these methods, recently employed in the determination of the critical temperature T_c for a system of weakly interacting homogeneous dilute Bose gas. We carry out the explicit LDE optimized calculations and also the infrared analysis of the relevant quantities involved in the determination of T_c in the large-N limit, when the relevant effective static action describing the system is extended to $O(N)$ symmetry. Then, using an efficient resummation method, we show how the LDE can exactly reproduce the known large-N result for T_c already at the first non-trivial order. Next, we consider the finite $N = 2$ case where, using similar resummation techniques, we improve the analytical results for the nonperturbative terms involved in the expression for the critical temperature allowing comparison with recent Monte Carlo estimates of them. To illustrate the method we have considered a simple geometric series showing how the procedure as a whole works consistently in a general case.

PACS numbers: 03.75.Hh, 05.30.Jp, 12.38.Cy, 11.10.Wx

I. INTRODUCTION

Scalar field theories are extremely important in the study of symmetry breaking and restoration in different branches of physics such as cosmology, particle physics and condensed matter physics, where they may represent inflatons, Higgs particles, quark–anti-quark bound states, Cooper pairs, bosonic atoms and molecules, respectively. In most cases the vacuum expectation value of those scalar fields represents an order parameter that signals phase transitions associated to symmetry breaking/restoration [1].

In general, one important problem we have to deal with when studying phase transitions in field theory regards the reliability of perturbation theory and its eventual breakdown. In this case, a nontrivial problem arises since nonperturbative methods must be used. This is the case in those physical situations involving a second order, or weakly first order phase transition, where we have to consider the problem of infrared (IR) divergences that become progressively more important as one approaches the critical temperature, from above or below, and that will unavoidably spoil any perturbative attempt to compute relevant quantities there. In those situations we must find appropriate methods to take into account the large IR corrections, present in the form of large field fluctuations. There is a variety of nonperturbative methods that can be used in order to account for these corrections, including the recent dynamical Boltzmann-like approach that deals directly with the large field fluctuations [2]. At the same time, the most common methods, at equilibrium, try to resum the leading IR corrections. This happens for example, through the use of ε-expansion techniques in order to compute corrections to the critical exponents that control the singular behavior of physical quantities near the critical point (as it is familiar from the theory of critical phenomena [3]), the large-N method and other approaches (for a review, see Ref. [4]).

An issue that has attracted considerable attention recently and that is associated to the perturbation theory breakdown problem is the study of how interactions alter the critical temperature (T_c) of Bose-Einstein condensation (BEC). Due to its nonperturbative nature, this is clearly a non-trivial problem. On the other hand, studies related to the BEC T_c problem are particularly important nowadays due the recent experimental realization of BEC on dilute atomic gases (for reviews, see for instance, Ref. [5]). The experimental achievement of BEC has induced many theoretical investigations which make use of methods developed to treat finite temperature quantum field theories.

*Electronic address: kneur@lpm.univ-montp2.fr
†Electronic address: marcus@lpm.univ-montp2.fr; [1] Permanent address
‡Electronic address: rudnei@dft.if.uerj.br

At the same time, due to the high experimental precision with which the parameters may be tuned, BEC experiments provide an important laboratory to test many methods as well as models developed to treat those theories (see, *e.g.*, Ref. [6]).

The studies concerning the equilibrium properties of BEC can be addressed by means of a non-relativistic effective theory described by a complex scalar field. In the dilute limit, which is the regime involved in those experiments, only two body interactions are important [5] and one may then consider the following $U(1)$ invariant finite temperature Euclidean action

$$S_E = \int_0^\beta d\tau \int d^3x \left\{ \psi^*(\mathbf{x},\tau) \left(\frac{d}{d\tau} - \frac{1}{2m}\nabla^2 \right) \psi(\mathbf{x},\tau) - \mu\psi^*(\mathbf{x},\tau)\psi(\mathbf{x},\tau) + \frac{2\pi a}{m} \left[\psi^*(\mathbf{x},\tau)\psi(\mathbf{x},\tau)\right]^2 \right\} , \tag{1.1}$$

where, in natural units, β is the inverse of the temperature, μ is the chemical potential and m represents the mass of the atoms. At the relevant low temperatures involved in BEC the internal degrees of freedom are unimportant and this can be taken as an effective model of hard core spheres with local interactions for which a represents the s-wave scattering length.

The field ψ can be decomposed into imaginary-time frequency modes $\psi_j(\mathbf{x},\omega_j)$, with discrete bosonic Matsubara frequencies $\omega_j = 2\pi j/\beta$, where j is an integer. Near the transition the chemical potential becomes very small as compared to the temperature ($|\mu| << T$) and, since the correlation length tends to infinity, the distances are large compared to the thermal wavelength $\lambda = \sqrt{2\pi\beta/m}$. Therefore, the non-zero Matsubara modes decouple and one is left with an effective action for the field zero modes ($j = 0$) given by [7]

$$S_{3d} = \beta \int d^3x \left\{ \psi_0^* \left(-\frac{1}{2m}\nabla^2 - \mu \right) \psi_0 + \frac{2\pi a}{m} \left[\psi_0^*\psi_0\right]^2 \right\} , \tag{1.2}$$

where ψ_0 stands for the field's zero mode. Recently, Arnold, Moore and Tomásik [8] have argued that when naively going from the original action (S_E) to the reduced action (S_{3d}) by ignoring the effects of non-zero frequency modes one misses the effects that short-distances and/or high-frequency modes have on long-distance physics. For the critical temperature of condensation as a function of the density ($T_c(n)$), at second order, these effects can be absorbed into a modification of the strengths of the relevant interactions which means that one should consider the more general form for the reduced effective action Eq. (1.2)

$$S_{\rm eff}[\psi_0,\psi_0^*] = \beta \int d^3x \left\{ \psi_0^* \left(-\mathcal{Z}_\psi \frac{1}{2m}\nabla^2 - \mu_3 \right) \psi_0 + \mathcal{Z}_a \frac{2\pi a}{m} \left[\psi_0^*\psi_0\right]^2 + \mathcal{O}\left[\psi_0^*\psi_0|\nabla\psi|^2, (\psi^*\psi)^3\right] \right\} + \beta F_{\rm vacuum} , \tag{1.3}$$

where $\mathcal{Z}_\psi$ is the wave-function renormalization function, μ_3 incorporates the mass renormalization function, $\mathcal{Z}_a$ incorporates the vertex renormalization function and $F_{\rm vacuum}$ represents the vacuum energy contributions coming from the integration over the nonstatic Matsubara modes. The $\mathcal{O}\left[\psi_0^*\psi_0|\nabla\psi_0|^2, (\psi_0^*\psi_0)^3\right]$ terms represent higher order interactions in the zero modes of the fields. As shown in Ref. [8], these terms will give contributions to the density of order-a^3 and higher and therefore do not enter the order-a^2 calculations considered here. By matching perturbative order-a^2 results obtained with the original action S_E and the general effective action $S_{\rm eff}$, the authors of Ref. [8] were able to show that the transition temperature for a dilute, homogeneous, three dimensional Bose gas can be expressed at next to leading order as

$$T_c = T_0 \left\{ 1 + c_1 a n^{1/3} + \left[c_2' \ln\left(a n^{1/3}\right) + c_2'' \right] a^2 n^{2/3} + \mathcal{O}\left(a^3 n\right) \right\} , \tag{1.4}$$

where T_0 is the ideal gas condensation temperature, $T_0 = 2\pi/m \left[n/\zeta(3/2)\right]^{2/3}$, n is the density, $\zeta(x)$ is the Riemann Zeta function and c_1, c_2' and c_2'' are numerical coefficients. A similar structure is also discussed in Ref. [9]. As far the numerical coefficients are concerned, the exact value, $c_2' = -64\pi\zeta(1/2)\zeta(3/2)^{-5/3}/3 \simeq 19.7518$, was obtained using perturbation theory [8]. On the other hand, the other two coefficients, c_1 and c_2'', are sensitive to the infrared sector of the theory and consequently cannot be obtained perturbatively, but they can, through the matching calculation, be expressed in terms of the two nonperturbative quantities κ and $\mathcal{R}$ which are, respectively, related to the number density $\langle\psi_0^*\psi_0\rangle$ and to the critical chemical potential μ_c, as shown below. The actual relation between the two nonperturbative coefficients and these physical quantities is given by [8]

$$c_1 = -128\pi^3 [\zeta(3/2)]^{-4/3}\kappa , \tag{1.5}$$

and

$$c_2'' = -\frac{2}{3}[\zeta(3/2)]^{-5/3} b_2'' + \frac{7}{9}[\zeta(3/2)]^{-8/3}(192\pi^3\kappa)^2 + \frac{64\pi}{9}\zeta(1/2)[\zeta(3/2)]^{-5/3}\ln\zeta(3/2)\,, \tag{1.6}$$

where b_2'', in Eq. (1.6), is

$$b_2'' = 32\pi\left\{\left[\frac{1}{2}\ln(128\pi^3) + \frac{1}{2} - 72\pi^2\mathcal{R} - 96\pi^2\kappa\right]\zeta(1/2) + \frac{\sqrt{\pi}}{2} - K_2 - \frac{\ln 2}{2\sqrt{\pi}}\left[\zeta(1/2)\right]^2\right\}\,, \tag{1.7}$$

with $K_2 = -0.13508335373$. The quantities κ and $\mathcal{R}$ are related to the zero Matsubara modes only. Therefore, they can be nonperturbatively computed directly from the reduced action $S_{\rm eff}$ which, as discussed in the numerous previous applications, can be written as

$$S_\phi = \int d^3x\left[\frac{1}{2}|\nabla\phi|^2 + \frac{1}{2}r_{\rm bare}\phi^2 + \frac{u}{4!}(\phi^2)^2\right]\,, \tag{1.8}$$

where $\phi = (\phi_1, \phi_2)$ is related to the original real components of ψ_0 by $\psi_0(\mathbf{x}) = \sqrt{mT/\mathcal{Z}_\psi}\,[\phi_1(\mathbf{x}) + i\phi_2(\mathbf{x})]$, $r_{\rm bare} = 2m\mu_3/\mathcal{Z}_\psi$ and $u = 48\pi amT\mathcal{Z}_a/{\mathcal{Z}_\psi}^2$. The vacuum contribution appearing in Eq. (1.3) will not enter in the specific calculation we do here and one has been omitted it from Eq. (1.8). In the large-N limit considered in the first part of this work, and also in Refs. [10, 11], the field ϕ in Eq. (1.8) is formally considered as having N components (ϕ_i, $i = 1, \ldots, N$). In this case, the Bose-Einstein condensate effective action Eq. (1.8) is the $N = 2$ special case of the general $O(N)$ invariant action.

The three dimensional effective theory described by Eq. (1.8) is super-renormalizable and requires only a mass counterterm to eliminate any ultraviolet divergence. In terms of Eq. (1.8), the quantities κ and $\mathcal{R}$ appearing in Eqs. (1.5) - (1.7) are defined by

$$\kappa \equiv \frac{\Delta\langle\phi^2\rangle_c}{u} = \frac{\langle\phi^2\rangle_u - \langle\phi^2\rangle_0}{u}\,, \tag{1.9}$$

and

$$\mathcal{R} \equiv \frac{r_c}{u^2} = -\frac{\Sigma(0)}{u^2}\,, \tag{1.10}$$

where the subscripts u and 0 in Eq. (1.9) mean that the density is to be evaluated in the presence and in the absence of interactions, respectively, and $\Sigma(0)$ is the self-energy with zero external momentum. Since these physical quantities are dependent on the zero modes their evaluation is valid, at the critical point, only when done in a nonperturbative fashion. As discussed in the next section, the relation between r_c and $\Sigma(0)$ comes from the Hugenholtz-Pines (HP) theorem at the critical point.

Eq. (1.4) is a general order-a^2 result with coefficients that, therefore, depend on nonperturbative physics via κ and $\mathcal{R}$. In principle, to evaluate these two quantities one may start from the effective three-dimensional theory, given by Eq. (1.8), and then employ any nonperturbative analytical or numerical technique.

When quantum corrections are taken into account, the full propagator for the effective three dimensional theory reads

$$G(p) = [p^2 + r + \Sigma_{\rm ren}(p)]^{-1}\,, \tag{1.11}$$

where p^2 represents the three momentum and $\Sigma_{\rm ren}(p)$ represents the renormalized self-energies. At the transition point ($p^2 = 0$), the system must have infinite correlation length and one then has

$$[G(0)]^{-1} = [r_c + \Sigma_{\rm ren}(0)] = 0\,. \tag{1.12}$$

This requirement leads to the Hugenholtz-Pines theorem result $r_c = -\Sigma_{\rm ren}(0)$. Since r_c is at least of order u it would be treated as a vertex in a standard perturbation type of calculation in which $G(p) = 1/p^2$ represents the bare

propagator. This shows that perturbation theory is clearly inadequate to treat the BEC problem at the transition due to the presence of infrared divergences. One must then recur to nonperturbative methods like the numerical lattice Monte Carlo simulations, the analytical $1/N$ or the linear δ expansion (LDE) [12] adopted in this work (see for instance Ref. [13] for earlier works on the method). The problem is highly nontrivial since the Hugenholtz-Pines theorem automatically washes out all momentum independent contributions, such as the one-loop tadpole diagrams, which constitute the leading order of most approximations. In practice, this means that the first nontrivial contributions start with two-loop momentum dependent self-energy terms. However, having reduced the original model, Eq. (1.1) to the effective three-dimensional one, Eq. (1.8), makes it easier to tackle those contributions since one no longer has the problem of summing over the Matsubara's frequencies, which is a hard task when the number of loops increases.

Recent numerical Monte Carlo applications [14, 15] have predicted values for c_1 which are close to 1.30 [1]. On the other hand, some analytical applications have predicted values such as ~ 2.90 obtained with a self-consistent resummation method [7], ~ 2.33 obtained with the $1/N$ expansion to leading order [10] and ~ 1.71 obtained with the same expansion to the next to leading order [11]. The LDE was first applied to order-δ^2 producing $c_1 \sim 3.06$ [17]. Recently, the calculation has been extended to order-δ^4 with the results ~ 2.45 at order-δ^3 and ~ 1.51 at order-δ^4 [18]. The coefficient c_2'' was evaluated with Monte Carlo techniques [14] and the predicted value obtained from those simulations is 75.7 ± 0.4. This quantity was also analytically evaluated with the LDE in Ref. [18], where the encountered numerical values are ~ 101.4, ~ 98.2 and ~ 82.9 at second, third and fourth orders respectively. An order-δ^2 application to ultra-relativistic gases has also been performed [19]. The LDE has been especially successful in treating scalar field theories at finite temperatures [20, 21] as well as finite temperature and density [22]. Several different applications performed with the LDE are listed in Ref. [18]. Recently, Braaten and Radescu [23] have also used the LDE, with different optimization prescriptions, to evaluate T_c both at large and finite N limits, while Kleinert [24] has used the variational perturbation theory, which is a variation of the LDE, obtaining the value $c_1 \sim 0.91 \pm 0.05$. Like we do here for the finite N case, he has considered up to order-δ^4 contributions which include five loop diagrams. However, none of those authors considers resummation techniques to accelerate convergence and do not evaluate the coefficient c_2'', that it is also computed in the present work.

As far as the application of the LDE to the determination of the BEC transition temperature is concerned, since the first papers making use of the LDE method to this problem [17, 18], an important question was raised and remained unanswered. This question regards the convergence properties of the method in this application for the BEC problem, which is in fact related to the convergence of the method in critical theories in general. Actually, this is a timely and important question regarding the applications of the LDE in field theories, since the first efforts have been concentrated mostly in the anharmonic oscillator problem at zero temperature, where rigorous LDE convergence proofs have been produced [25, 26, 27, 28]. The extension to the finite temperature domain was also considered by Duncan and Jones [29], who used the anharmonic oscillator partition function. Only very recently a convergence proof has been extended, but for a particular perturbative series case, to asymptotically free renormalizable quantum field theories at zero temperature [30]. Here, as in a previous paper from us, Ref. [31], our interest is to probe convergence in the vicinity of a phase transition, such as for the Bose-Einstein condensation problem presented above. This study should also settle the questions regarding the correctness of our original LDE applications [17, 18], since by showing convergence in the large-N case we also establish the reliability of our finite N results, as originally studied in those investigations. The LDE convergence in the large-N extension of the BEC problem has also been recently addressed by Braaten and Radescu [23]. The differences between their approach and ours will be discussed in some detail in the text.

The literature shows [28, 32, 33] that in most applications it is possible to establish simple relations between the LDE and other nonperturbative methods already at order-δ where one-loop diagrams are present. In fact, one can show that in those cases the LDE either exactly reproduces $1/N$ results or produce very close numerical results. Here, the BEC problem poses an additional difficulty since, as discussed above, the first non-trivial contributions start at the two-loop level in the self-energies. As we shall see, it is not easy in this case to establish simple analytical relations for the quantities being computed, like those given *e.g.* in Refs. [28, 32, 33], and the problem must be treated differently. However, as we are going to show in the coming sections, our numerical results, improved with an efficient resummation technique exactly converge in the large-N limit and seems to also converge in the arbitrary N case.

This paper is organized as follows. In Sec. II we briefly recall the LDE method and present the interpolated version of the action Eq. (1.8) to be studied throughout the paper, following the recent applications performed in Refs. [17, 18]. In Sec. III, we carry out the formal evaluation of $\langle \phi^2 \rangle_u$ in three different ways. The first is the usual order by order type of calculation, which is familiar from perturbative calculations, and is in fact the only possible

[1] See Ref. [16] for an extension of these works to the $O(1)$ and $O(4)$ cases.

one for the realistic finite N case. The second uses the type of resummation familiar from nonperturbative methods such as Hartree and the $1/N$ approximations. These two procedures generate two series for the large-N limit of $\langle\phi^2\rangle_u$ (in which case ϕ in Eq. (1.8) is extended to N components) whose coefficients, which are numerically obtained, can be usefully compared as a cross check, helping to establish the numerical reliability of the finite N series. In the same section, we also consider the asymptotic infrared and ultraviolet behavior of the series which, as we shall see, is a very useful approximation allowing at the same time a fully analytical analysis. In Sec. IV we first examine the LDE optimized perturbation procedure in a general case, considering a simple geometric series in order to get insight regarding the convergence structure of the optimal results. Then, the large-N BEC series are optimized and a resummation technique which accelerates convergence is introduced. By taking the large-N result for c_1 (obtained in Ref. [10]) as a reference value we proceed with the investigation of convergence, showing that the LDE together with the resummation technique can exactly reproduce the large-N result already at the first non-trivial order, provided that it is applied to a specific approximation fully exploiting the infrared limit properties. Having explicitly shown the LDE convergence properties within a limit where an exact result exists we turn our attention, in Sec. V, to the realistic finite N case where no similar infrared approximation is available. Using the same resummation method, the order-δ^4 results for c_1 and c_2'' obtained in Ref. [18] are improved and the results obtained seem to converge to the lattice Monte Carlo estimates of Ref. [14]. Our conclusions are presented in Sec. VI. For completeness and comparison purposes we also include two appendixes, one where the original large-N derivation is reviewed and another one to detail useful properties of the large order behavior of the LDE.

II. LDE AND THE INTERPOLATED EFFECTIVE SCALAR THEORY FOR BEC

Let us start our work by reviewing the application of the LDE method to our problem. The LDE was conceived to treat nonperturbative physics while staying within the familiar calculation framework provided by perturbation theory. In practice, this can be achieved as follows. Starting from an action S one performs the following interpolation

$$S \to S_\delta = \delta S + (1-\delta) S_0(\eta) \,, \tag{2.1}$$

where S_0 is the soluble quadratic action, added by an (optimizable) mass term η, and δ is an arbitrary parameter. The above modification of the original action somewhat reminds the usual trick consisting of adding and subtracting a mass term to the original action. One can readily see that at $\delta = 1$ the original theory is retrieved, so that δ actually works just as a bookkeeping parameter. The important modification is encoded in the field dependent quadratic term $S_0(\eta)$ that, for dimensional reasons, must include terms with mass dimensions (η). In principle, one is free to choose these mass terms and within the Hartree approximation they are replaced by a direct (or tadpole) type of self-energy before one performs any calculation. In the LDE they are taken as being completely arbitrary mass parameters, which will be fixed at the very end of a particular evaluation by an optimization method. One then formally pretends that δ labels interactions so that S_0 is absorbed in the propagator whereas δS_0 is regarded as a quadratic interaction. So, one sees that the physical essence of the method is the traditional dressing of the propagator to be used in the evaluation of physical quantities very much like in the Hartree case. What is different between the two methods is that, within the LDE the propagator is completely arbitrary, constrained only to cope with the so-called direct terms (*i.e.* tadpoles) within the Hartree approximation. So, within the latter approximation the relevant contributions are selected according to their topology from the start.

Within the LDE one calculates in powers of δ as if it was a small parameter. In this respect the LDE resembles the large-N calculation since both methods use a bookkeeping parameter which is not a physical parameter like the original coupling constants and within each method one performs the calculations formally working as if $N \to \infty$ or $\delta \to 0$, respectively. Finally, in both cases the bookkeeping parameters are set to their original values at the end which, in our case, means $\delta = 1$. However, quantities evaluated at any finite LDE order from the dressed propagator will depend explicitly on η, unless one could perform a calculation to all orders. Up to this stage the results remain strictly perturbative and very similar to the ones which would be obtained via a true perturbative calculation. It is now that the freedom in fixing η generates nonperturbative results. Since η does not belong to the original theory one may require that a physical quantity $\Phi^{(k)}$ calculated perturbatively to order-δ^k be evaluated at the point where it is less sensitive to this parameter. This criterion, known as the Principle of Minimal Sensitivity (PMS), translates into the variational relation [34]

$$\frac{d\Phi^{(k)}}{d\eta}\Big|_{\bar{\eta},\delta=1} = 0 \,. \tag{2.2}$$

The optimum value $\bar{\eta}$ which satisfies Eq. (2.2) must be a function of the original parameters including the couplings, which generates the nonperturbative results. Another optimization procedure, known as Fastest Apparent Convergence criterion (FAC) (see also Ref. [34]), may also be employed. It requires, from the k-th coefficient of the perturbative expansion

$$\Phi^{(k)} = \sum_{i=0}^{k} c_i \delta^i \, , \tag{2.3}$$

that

$$\left[\Phi^{(k)} - \Phi^{(k-1)}\right]\Big|_{\delta=1} = 0 \, , \tag{2.4}$$

which is just equivalent to taking the k-th coefficient (at $\delta = 1$) in Eq. (2.3) equal to zero. For the interested reader Refs. [17, 18, 19, 20, 21, 22, 23, 25, 26, 27, 28, 29, 30, 31, 32, 33] provide an extensive (but far from complete) list of successful applications of the method to different problems.

It is important to recall that the basic reason for the convergence of the LDE method in the quantum mechanics case (anharmonic oscillator energy levels typically) [25, 26, 27, 28] relies on the fact that the LDE modifies perturbative expansions in such a way that the PMS or FAC optimized values of the initially arbitrary mass parameter (the equivalent of η here) essentially follow, at large perturbative orders, a pattern of rescaling this mass with the perturbative order, which is such as to compensate the generic factorial growth [35] of the original perturbative expansion coefficients at large orders. As we will see in Sec III, in the present BEC case the relevant perturbative expansions do not exhibit factorially growing coefficients, but nevertheless the reasons for convergence of the LDE share some similarities with the latter cases, since the LDE followed by PMS also introduces at sufficiently large order a certain scaling behavior with the perturbative order, in such a way as to modify (extend) the convergence radius of the original perturbative series.

Let us now write the interpolated version of the effective model described by Eq. (1.8). Before doing that let us rewrite $r_{\rm bare} = r + A$ where A is a mass counterterm coefficient needed to remove the UV divergence from the self-energy. This counterterm is the only one effectively needed within the modified minimal subtraction ($\overline{\rm MS}$) renormalization scheme adopted here for the evaluation of the relevant Feynman diagrams contributing to the self-energy, as explicitly shown in Ref. [18]. Then, one can choose

$$S_0 = \frac{1}{2}\left[|\nabla\phi|^2 + \eta^2\phi^2\right] \, , \tag{2.5}$$

obtaining

$$S_\delta = \int d^3x \left[\frac{1}{2}|\nabla\phi|^2 + \frac{1}{2}\eta^2\phi^2 + \frac{\delta}{2}(r-\eta^2)\phi^2 + \frac{\delta u}{4!}(\phi^2)^2 + \frac{\delta}{2}A_\delta\phi^2\right] \, , \tag{2.6}$$

where A_δ represents the renormalization mass counterterm for the interpolated theory, which depends on the parameters η and δ. It is important to note that by introducing only extra mass terms in the original theory the LDE does not alter the polynomial structure and, hence, the renormalizability of a quantum field theory. In practice, the original counterterms change in an almost trivial way so as to absorb the new η and δ dependence. The compatibility of the LDE with the renormalization program has been shown in the framework of the $O(N)$ scalar field theory at finite temperatures, in the first work of Ref. [21], showing that it consistently takes into account anomalous dimensions in the critical regime. Note also that we have treated r as an interaction, since this quantity has a critical value (r_c) that is at least of order δ.

Requiring the original system to exhibit infinite correlation length at the critical temperature, means that, at T_c and $\delta = 1$ (the original theory), the full propagator $G^{(\delta)}(p)$, given by

$$G^{(\delta)}(p) = \left[p^2 + \eta^2 + \delta r - \delta\eta^2 + \Sigma^{(\delta)}_{\rm ren}(p)\right]^{-1} \, , \tag{2.7}$$

must satisfy $G^{(\delta)}(0)^{-1} = 0$. This requirement implies

$$\delta r_c^{(\delta)} = -\Sigma^{(\delta)}_{\rm ren}(0) \, , \tag{2.8}$$

which is equivalent to the Hugenholtz-Pines theorem applied to the LDE.

III. LDE EVALUATION OF $\langle\phi^2\rangle_u^{(\delta)}$ IN THE LARGE-N LIMIT

Let us now turn our attention to the explicit LDE evaluation of $\langle\phi^2\rangle_u^{(\delta)}$ in the large-N limit. In practice, the large-N evaluation can be performed in different fashions which include the conventional order by order perturbative evaluation and the more economical closed form evaluation in which the whole large-N series is resummed. The first, purely perturbative method in the standard Feynman graph way is also the only possible one concerning the finite N calculations, where different classes of diagrams contribute. The second technique is usually employed in approximations such as Hartree and $1/N$ where it is possible to sum a certain class of graphs based on the type of loop terms they contain. Having resummed a given class, one may easily obtain a perturbative result by expanding the series to a given order in δu. Of course, both methods must lead to equivalent analytical results but, as we shall see, the final numerical results can be different at high perturbative orders. This is due to the fact that both perturbative expansions contain coefficients numerically produced. Since our optimization procedures may be sensitive to the numerical precision of those coefficients it will be instructive to compare them in detail. Finally, one can move one step further by obtaining a series with exact coefficients that allows for a fully analytical investigation. This is made possible by considering an approximation which avoids complicated integrals appearing in the exact calculation due to the presence of dressed propagators in terms of self-energies, which are usually cumbersome beyond some given order. Such a simpler series, with exact coefficients, is obtained if one considers typically the physically motivated deep infrared behavior of the dressed scalar propagators. In this section we explore these three possible evaluations.

A. Standard Perturbative Evaluation of $\langle\phi^2\rangle_u^{(\delta)}$

Let us evaluate $\langle\phi^2\rangle_u^{(\delta)}$ in the usual perturbative way. The relevant contributions, in the large-N limit, are shown in Fig. 1. Using the full propagator one may write this quantity, at the critical point, as

$$\langle\phi^2\rangle_u^{(\delta)} = \sum_{i=1}^{N}\langle\phi_i^2\rangle_u^{(\delta)} = N\int\frac{d^3p}{(2\pi)^3}G^{(\delta)}(p) = \int\frac{d^3p}{(2\pi)^3}\frac{N}{p^2+(\eta^*)^2}\left[1+\frac{\delta r_c^{(\delta)}+\Sigma_{\rm ren}^{(\delta)}(p)}{p^2+(\eta^*)^2}\right]^{-1}, \tag{3.1}$$

where $\eta^* = \eta\sqrt{1-\delta}$. Note that with this prescription one only has to evaluate diagrams which would appear in a usual perturbative calculation since the quadratic $\delta\eta^2$ vertex is automatically taken into account when η^* is expanded to the relevant order in δ.

One can express the large-N calculation more conveniently, in the generalization of Eq. (1.8) to $O(N)$ symmetry, by considering $u = u'/N$. In this case the nontrivial contributions, in the large-N limit and expanded to LDE order k, are given by

$$\langle\phi^2\rangle_u^{(k)} = N\int\frac{d^3p}{(2\pi)^3}\frac{1}{p^2+(\eta^*)^2} - N\int\frac{d^3p}{(2\pi)^3}\frac{[\Sigma^{(n)}(p)-\Sigma^{(n)}(0)]}{[p^2+(\eta^*)^2]^2}, \tag{3.2}$$

where we have used Eq. (2.8) and $\Sigma^{(n)}$ denotes the n-bubble self-energy given by

$$\Sigma^{(n)}(p) = -\frac{2}{N}\left(-\frac{\delta u'}{6}\right)^{n+1}\int\frac{d^3l}{(2\pi)^3}\frac{1}{(l^2+(\eta^*)^2)}\left[\int\frac{d^3s}{(2\pi)^3}\frac{1}{(s^2+(\eta^*)^2)}\frac{1}{[(s+p-l)^2+(\eta^*)^2]}\right]^n, \tag{3.3}$$

which is then of order $k = n+1$ in δ. Note that the mass counterterm is a redundant quantity in the evaluation of $\langle\phi^2\rangle_u^{(k)}$ because this quantity depends on the difference

$$\Sigma_{\rm ren}^{(n)}(p) - \Sigma_{\rm ren}^{(n)}(0) = [\Sigma_{\rm div}^{(n)}(p) + \Sigma_{\rm ct}^{(n)}(p)] - [\Sigma_{\rm div}^{(n)}(0) + \Sigma_{\rm ct}^{(n)}(0)], \tag{3.4}$$

where $\Sigma_{\rm div}^{(n)}(p)$ is the divergent self-energy. For a general renormalizable theory, the quantity $\Sigma_{\rm ct}^{(n)}(p)$ represents all counterterms associated with the parameters of the theory (such as masses and coupling constants) as well as the wave-function counterterm associated with any eventual momentum dependent pole. At the same time, $\Sigma_{\rm ct}^{(n)}(0)$ involves the same counterterms except for the wave-function one. However, as we have already emphasized previously, in the three-dimensional case the only type of primitive divergence requires only a mass counterterm, which is the same for

$\Sigma^{(n)}_{\rm div}(p)$ and $\Sigma^{(n)}_{\rm div}(0)$. This means that in our case, $\Sigma^{(n)}_{\rm div}(p) - \Sigma^{(n)}_{\rm div}(0)$ is always a finite quantity. It turns out that this quantity is also scale independent as discussed in Ref. [18]. Since however the individual contribution $\Sigma^{(n)}_{\rm div}(p)$ contain a divergence, we regularize all diagrams with dimensional regularization in arbitrary dimensions $d = 3 - 2\epsilon$, where in the modified minimal subtraction ($\overline{\rm MS}$) renormalization scheme, the momentum integrals can be written as

$$\int \frac{d^3p}{(2\pi)^3} \to \left(\frac{e^{\gamma_E} M^2}{4\pi}\right)^{\epsilon} \int \frac{d^dp}{(2\pi)^d} \,, \tag{3.5}$$

where M is an arbitrary mass scale and $\gamma_E \simeq 0.5772$ is the Euler-Mascheroni constant.

Then, from the use of standard Feynman parameters for the integrals over momenta, we can write the general form for each of the two terms in $\langle\phi^2\rangle^{(k)}_u$, Eq. (3.2), that depend on the self-energy. The first of such term can be expressed as

$$\begin{aligned}
-N\int \frac{d^3p}{(2\pi)^3}\frac{\Sigma^{(n)}(p)}{[p^2+(\eta^*)^2]^2} &= \frac{(-\delta u')^{n+1}}{3(6\eta^*)^n}\frac{\Gamma[n(1/2+\epsilon)+2\epsilon]}{(4\pi)^{3/2(n+2)}}\left(\frac{e^{\gamma}M^2}{(\eta^*)^2}\right)^{\epsilon(n+2)} \\
&\times \int_0^1 d\chi\chi(1-\chi)^{-3/2+\epsilon+n(1/2+\epsilon)}\int_0^1 d\gamma(1-\gamma)^{n(1/2+\epsilon)-1}[\gamma(1-\gamma)]^{1/2-\epsilon-n(1/2+\epsilon)} \\
&\times \int_0^1 d\alpha_1[\alpha_1(1-\alpha_1)]^{-(1/2+\epsilon)}\ldots\int_0^1 d\alpha_n[\alpha_n(1-\alpha_n)]^{-(1/2+\epsilon)} \\
&\times \int_0^1 d\beta_1\beta_1^{n-2}[\beta_1(1-\beta_1)]^{-1/2}\int_0^1 d\beta_2\beta_2^{n-3}[\beta_1\beta_2(1-\beta_2)]^{-1/2}\ldots \\
&\times \int_0^1 d\beta_{n-1}[\beta_1\beta_2\ldots\beta_{n-1}(1-\beta_{n-1})]^{-1/2}\mathcal{F}(\chi,\gamma,\alpha_i,\beta_j) \,,
\end{aligned} \tag{3.6}$$

where

$$\mathcal{F}(\chi,\gamma,\alpha_i,\beta_j) = \left\{\chi + \frac{(1-\chi)}{\gamma(1-\gamma)}\left[\gamma + (1-\gamma)\left(\frac{(1-\beta_1)}{\alpha_1(1-\alpha_1)} + \frac{\beta_1(1-\beta_2)}{\alpha_2(1-\alpha_2)} + \ldots + \frac{(\beta_1\beta_2\ldots\beta_{n-1})}{\alpha_n(1-\alpha_n)}\right)\right]\right\}^{-[n(1/2+\epsilon)+2\epsilon]} . \tag{3.7}$$

At the same time, the $p = 0$ term is given by

$$\begin{aligned}
-N\int \frac{d^3p}{(2\pi)^3}\frac{\Sigma^{(n)}(0)}{[p^2+(\eta^*)^2]^2} &= \frac{(-\delta u')^{n+1}}{3(6\eta^*)^n}\frac{\Gamma[n(1/2+\epsilon)+\epsilon-1/2]}{8\pi(4\pi)^{3/2(n+1)}}\left(\frac{e^{\gamma}M^2}{(\eta^*)^2}\right)^{\epsilon(n+1)} \\
&\times \int_0^1 d\gamma(1-\gamma)^{n(1/2+\epsilon)-1}[\gamma(1-\gamma)]^{1/2-\epsilon-n(1/2+\epsilon)} \\
&\times \int_0^1 d\alpha_1[\alpha_1(1-\alpha_1)]^{-(1/2+\epsilon)}\ldots\int_0^1 d\alpha_n[\alpha_n(1-\alpha_n)]^{-(1/2+\epsilon)} \\
&\times \int_0^1 d\beta_1\beta_1^{n-2}[\beta_1(1-\beta_1)]^{-1/2}\int_0^1 d\beta_2\beta_2^{n-3}[\beta_1\beta_2(1-\beta_2)]^{-1/2}\ldots \\
&\times \int_0^1 d\beta_{n-1}[\beta_1\beta_2\ldots\beta_{n-1}(1-\beta_{n-1})]^{-1/2}\mathcal{G}(\gamma,\alpha_i,\beta_j) \,,
\end{aligned} \tag{3.8}$$

where

$$\mathcal{G}(\gamma,\alpha_i,\beta_j) = \left\{\frac{1}{\gamma(1-\gamma)}\left[\gamma + (1-\gamma)\left(\frac{(1-\beta_1)}{\alpha_1(1-\alpha_1)} + \frac{\beta_1(1-\beta_2)}{\alpha_2(1-\alpha_2)} + \ldots + \frac{(\beta_1\beta_2\ldots\beta_{n-1})}{\alpha_n(1-\alpha_n)}\right)\right]\right\}^{-[n(1/2+\epsilon)+\epsilon-1/2]} . \tag{3.9}$$

It is not very difficult to see, by counting the superficial degree of divergence in Eq. (3.3), that the only ultraviolet divergence shows up in the one-bubble ($n = 1$) contribution. In Eq. (3.6) the UV divergence for this case hides in the term $\chi(1-\chi)^{-3/2+\epsilon+n(1/2+\epsilon)}$ and appears explicitly upon integration by parts over χ. After that one can take the

usual expansion in powers of ϵ and perform a numerical integration over the Feynman parameters to obtain for the first, non-vanishing, term in Eq. (3.6) the result [17]

$$-N\int_p \frac{\delta^2\Sigma^{(1)}(p)}{[p^2+(\eta^*)^2]^2} = \delta^2\frac{(u')^2}{\eta^*}\frac{1}{18(8\pi)^3}\left[\frac{1}{\epsilon}+6\ln\left(\frac{M}{2\eta^*}\right)+2-4\ln 2\right] . \tag{3.10}$$

In the $p=0$ case the pole shows up in the gamma function which becomes $\Gamma(2\epsilon)$ for $n=1$. Integration yields

$$N\int_p \frac{\delta^2\Sigma^{(1)}(0)}{[p^2+(\eta^*)^2]^2} = -\delta^2\frac{(u')^2}{\eta^*}\frac{1}{18(8\pi)^3}\left[\frac{1}{\epsilon}+6\ln\left(\frac{M}{2\eta^*}\right)+2+4\ln(2/3)\right] . \tag{3.11}$$

The last two equations also reproduce the results found analytically in Refs. [17, 36]. As already mentioned, although Eq. (3.10) and Eq. (3.11) diverge, their sum is finite and scale independent. Together, they give the contribution

$$-N\int_p \frac{\delta^2[\Sigma^{(1)}(p)-\Sigma^{(1)}(0)]}{[p^2+(\eta^*)^2]^2} = -\delta^2\frac{(u')^2}{\eta^*}\frac{1}{18(8\pi)^3}4\ln(4/3) . \tag{3.12}$$

All higher loop contributions are finite and one can safely take $\epsilon=0$ in Eqs. (3.6) and (3.8). Note that in the above perturbative series, that is generated order by order from the standard Feynman graph procedure, the first non-trivial contributions start at order δ^2u^2, due to the fact that the first order expansion term, linear in δu (*i.e.* $n=0$ in Eq. (3.3)), is automatically canceled as a consequence of the Hugenholtz-Pines theorem, Eq. (2.8). The number of Feynman variables at each order is $k+2$ for Eq. (3.6) and $k+1$ for Eq. (3.8). We then get the order-δ^{20} result in the large-N limit

$$\langle\phi^2\rangle_u^{(20)} = -\frac{N\eta^*}{4\pi}+\delta\frac{uN}{3}\sum_{i=1}^{19}C_i\left(-\frac{\delta uN}{6\eta^*}\right)^i+\mathcal{O}(\delta^{21}) . \tag{3.13}$$

Except for the first coefficient, where we have the exact result from Eq. (3.12), all the other coefficients for $i\geq 2$ can only be obtained numerically. One well known numerical routine that can be used to evaluate the i-dimensional integrals over the Feynman parameters in Eqs. (3.6) and (3.8) is the Monte Carlo multidimensional integration routine VEGAS [37]. However, one should bear in mind that VEGAS may not be so reliable for a very large number of dimensions, since VEGAS, as a Monte-Carlo integration method, inherently makes use of finite numbers of points and iterations and these cannot be increased indefinitely in practice in order to improve precision. So for integrals with a *very* large number of dimensions (for example the last coefficient C_{19} involve a 39-dimensional integral) the VEGAS may lead to wrong estimates for both the numerical value of the integral and the corresponding error bar estimate obtained from the code (which also depends on the number of points and iterations used). Fortunately, as we will see below, all the terms contributing at large N can be computed alternatively in a much easier way (and to arbitrary precision) in terms of one-dimensional integrals, thus assuring a much better precision for the results and we do not need to worry about any specific detail of any numerical routine to evaluate Eqs. (3.6) and (3.8). The coefficients obtained this way, which we denote by J_i and are given in the following Subsection, will be the results used in all of our large-N calculations. These J_i coefficients can be contrasted then to the results obtained from e.g. with VEGAS, that we show here for illustrative purposes only, obtained using 10^4 points with 100 iterations fixed VEGAS parameters: $C_1=(7.249\pm0.001)\times10^{-5}$, $C_2=(2.050\pm0.003)\times10^{-6}$, $C_3=(6.32\pm0.01)\times10^{-8}$, $C_4=(2.048\pm0.003)\times10^{-9}$, $C_5=(6.85\pm0.01)\times10^{-11}$, $C_6=(1.709\pm0.002)\times10^{-12}$, $C_7=(3.561\pm0.006)\times10^{-14}$, $C_8=(6.48\pm0.01)\times10^{-16}$, $C_9=(1.063\pm0.002)\times10^{-17}$, $C_{10}=(1.560\pm0.005)\times10^{-19}$, $C_{11}=(2.59\pm0.04)\times10^{-21}$, $C_{12}=(5.00\pm0.09)\times10^{-23}$, $C_{13}=(9\pm2)\times10^{-26}$, $C_{14}=(5\pm1)\times10^{-28}$, $C_{15}=(5\pm1)\times10^{-30}$, $C_{16}=(1\pm7)\times10^{-33}$, $C_{17}=(2.3\pm0.6)\times10^{-34}$, $C_{18}=(2\pm2)\times10^{-37}$ and $C_{19}=(5\pm5)\times10^{-39}$. Note that starting with C_{13} the errors increase considerably as the dimension increases, as expected with a fixed number of VEGAS parameters.

B. Closed Form Evaluation of $\langle\phi^2\rangle_u^{(\delta)}$

Let us now write the whole large-N perturbative series in a closed form which resembles the usual $1/N$ resummation of Feynman graphs. For completeness and comparison purposes we re-derive, in Appendix A, the original large-N result found by Baym, Blaizot and Zinn-Justin [10]. Note, as already emphasized, that one basic difference between

the original large-N calculation and the LDE one is that the latter automatically introduces an infrared regulated propagator, from the explicit mass term η. Apart from its main purpose of defining in that way the relevant LDE series in $\delta u/\eta$, cf. Eq. (3.13), this also has the advantage of explicitly regularizing the intrinsic infrared divergence of the corresponding expression of T_c in the original calculations [10, 11]. However, similarly with the latter, there still remain some subtleties with this closed (resummed) form of the perturbation series, related to the fact that the integrals over momenta are not absolutely (UV) convergent, as we shall examine below. Thus, after applying the Hugenholtz-Pines theorem, and summing all the leading large-N contributions shown in Fig. 1, one obtains for the expression equivalent to Eq. (3.2) the result

$$\begin{aligned}\langle\phi^2\rangle_u^{(\delta)} &= N\int\frac{d^3p}{(2\pi)^3}\frac{1}{p^2+(\eta^*)^2} \\ &- \frac{\delta uN}{3}\int\frac{d^3\,p}{(2\pi)^3}\,\frac{d^3\,k}{(2\pi)^3}\,\frac{1}{[p^2+(\eta^*)^2]^2}\,\left[1+\frac{\delta uN}{6}B(k,\eta^*)\right]^{-1}\,\left[\frac{1}{(k+p)^2+(\eta^*)^2}-\frac{1}{k^2+(\eta^*)^2}\right]\,, \quad (3.14)\end{aligned}$$

where

$$B(k,\eta^*)=\int\,\frac{d^3q}{(2\pi)^3}\,\frac{1}{[q^2+(\eta^*)^2]\,[(k+q)^2+(\eta^*)^2]}\,=\frac{1}{4\pi k}\,\arctan\left(\frac{k}{2\eta^*}\right)\,, \quad (3.15)$$

with $k\equiv|\mathbf{k}|$ and similarly for p, q in Euclidean space. Contrary to the corresponding expression in the massless case $\eta=0$ (see Appendix A), here it appears not possible to integrate exactly Eq. (3.14) due to the non-trivial dependence in k and η^* of the resummed propagator $B(k,\eta^*)$. But one can at least still do exactly the first integral over the momentum p. In Eq. (3.14), the integral over p is finite in $d=3$, and can be easily performed to give

$$\langle\phi^2\rangle_u^{(\delta)}=-\frac{N\eta^*}{4\pi}-\frac{\delta uN}{3}\frac{1}{(8\pi\eta^*)}\int\frac{d^3k}{(2\pi)^3}\left[1+\frac{\delta uN}{6}B(k,\eta^*)\right]^{-1}\,\left[\frac{1}{k^2+4(\eta^*)^2}-\frac{1}{k^2+(\eta^*)^2}\right]\,, \quad (3.16)$$

while the remaining k-integral can be performed numerically. After a little algebra one gets

$$\langle\phi^2\rangle_u^{(\delta)}=-\frac{N\eta^*}{4\pi}+\frac{uN}{96\pi^2}+\delta\frac{uN}{3}\sum_{i=1}^{\infty}J_i\left(-\frac{\delta uN}{6\eta^*}\right)^i\,, \quad (3.17)$$

where the J_i coefficients are given by

$$J_i=\frac{3}{16\pi^3}\left(\frac{1}{8\pi}\right)^i\int_0^\infty dz\frac{z^2}{(z^2+1)(z^2+4)}[A(z)]^i\,, \quad (3.18)$$

with

$$A(z)=\frac{2}{z}\arctan\frac{z}{2}\,, \quad (3.19)$$

and $z=k/\eta^*$. Analytically, the two ways we have presented for obtaining the perturbative evaluation of $\langle\phi^2\rangle_u^{(\delta)}$ are expected to be equivalent and any difference may only arise from the numerical evaluation of the C_i and J_i coefficients. In this respect one expects J_i, which are evaluated from one dimensional integrals, to be more accurate than C_i and it will be instructive to compare both results. We have numerically evaluated J_i with both MATHEMATICA [38] and Maple, where we can compute the integrals with arbitrary precision, using diverse integration routines available in both, in order to check the reliability of the results. The first nineteen values obtained are $J_1=7.24858\times10^{-5}$, $J_2=2.04919\times10^{-6}$, $J_3=6.32139\times10^{-8}$, $J_4=2.04829\times10^{-9}$, $J_5=6.85295\times10^{-11}$, $J_6=2.3454\times10^{-12}$, $J_7=8.16524\times10^{-14}$, $J_8=2.88069\times10^{-15}$, $J_9=1.02726\times10^{-16}$, $J_{10}=3.69589\times10^{-18}$, $J_{11}=1.33955\times10^{-19}$, $J_{12}=4.88611\times10^{-21}$, $J_{13}=1.79203\times10^{-22}$, $J_{14}=6.60406\times10^{-24}$, $J_{15}=2.44405\times10^{-25}$, $J_{16}=9.07903\times10^{-27}$, $J_{17}=3.38400\times10^{-28}$, $J_{18}=1.26514\times10^{-29}$ and $J_{19}=4.74288\times10^{-31}$. Comparing C_i to J_i one sees that the multi-dimensional VEGAS routine produces accurate results up to $i=5$ but the values quickly deteriorate at large orders. This is a consequence that the VEGAS routine does not handle well integrals with a too large number of dimensions, for relatively (and computationally viable) small number of points and iterations, as explained at the

end of Sec. III.A. Therefore, in this work, we shall consider only the series with the more accurate J_i coefficients, as computed from Eq. (3.18).

However, one notes that Eq. (3.17) displays a more significant difference with respect to the "direct" perturbative series in Eq. (3.13), which is due to the presence of the extra first order term in δu, independent of η. Remark that this contribution is just the *opposite*, in sign, of the exact large-N result [10] (see Eq. (A11) in Appendix A). This apparent difference between the two approaches to the large-N perturbative series deserves a detailed discussion to which we now turn our attention on. In fact, the above difference is only a consequence of integrating expression (3.14) over p first. Namely, if performing the expansion in powers of δ, and then integrating first over k in Eq. (3.14) (which is formally equivalent to what is done in the standard perturbative order-by-order graphical approach in the previous subsection), the linear term in δu automatically cancels out. More precisely one obtains in this case an integral of the type (ξ just denotes an arbitrary mass parameter here, that is equal to η^* in the LDE calculation)

$$\sim N\, u\delta \int \frac{d^3\, k}{(2\pi)^3} \left(\frac{1}{(k+p)^2+\xi^2} - \frac{1}{k^2+\xi^2} \right) , \tag{3.20}$$

and in dimensional regularization the two terms in the bracket just cancel out, as can be seen by making a shift $k \to k-p$ in the first term. (One can also check with a standard cutoff regularization that the integral in Eq. (3.20) gives a zero result, though it is a less immediate calculation). Therefore depending on the order in which the two integrals in Eq. (3.14) are performed one may get different results, which is precisely the manifestation of an ambiguity due to the fact that the integrals are not absolutely (UV) convergent, as pointed out in Refs. [10, 11]. Actually, this problem is more basically rooted in the fact that in obtaining Eq. (3.14) one has formally resummed a series containing UV divergences, considering, e.g., the separate contributions in the last parenthesis of Eqs. (3.14) (see also Eqs. (A1) and (A2) in Appendix A). Therefore, the actual point is that one is not allowed (in principle) to exchange the perturbative, all order summation, with integration, which in our calculation is reflected in the different resulting perturbative series. Going back to the standard perturbative expansion, as performed in the previous subsection (Eqs. (3.2)–(3.8)) the perturbative parameter expansion in powers of δ is made first, and the UV divergence (which only appears at first non-trivial order $\delta^2 u^2$ as discussed there) may be taken care of by the standard renormalization. On the other hand, if we formally re-expand Eq. (3.14) in a power series in u, we can immediately see that the integral defining the coefficient of the first order term linear in $u\delta$, originating from $[1+(\delta u N/6)B(k,\eta^*)]^{-1} \sim 1$, has momenta routing that cannot be consistent with the actual perturbative graph: rather, considering for instance the first term of the last parenthesis in Eq. (3.14), one should have $p+k \to p$ for consistency (see Fig. 1), since this first order term in δu implies that the resummed propagator (dotted line) is pinched to a point, so that there is no k-momentum flow. This would give again a zero result for the coefficient of u, just for the same reasons as Eq. (3.20) is vanishing, while formally performing the integral with $p+k$ instead gives the $N\, u/(96\pi^2)$ term [2]. To summarize, while it will appear very convenient to formally perform the integral over p first in Eq.(3.14), it is only consistent provided one subtracts the spurious linear term from the naive result, Eq. (3.17). The correct perturbative series thus reads

$$\langle \phi^2 \rangle_u^{(\delta)} = -\frac{N\eta^*}{4\pi} + \delta \frac{uN}{3} \sum_{i=1}^{\infty} J_i \left(-\frac{\delta u N}{6\eta^*} \right)^i , \tag{3.21}$$

which has the same form as Eq. (3.13). An expression similar to Eq. (3.21) was also found by Braaten and Radescu in Ref. [23].

C. Asymptotic infrared and ultraviolet behavior of $\langle \phi^2 \rangle_u^{(\delta)}$

Before considering the relevant BEC perturbation series, Eq. (3.13), or equivalently Eq. (3.21), in the large-N limit, let us recall some expected general properties of the large order perturbative expansions, as seen from a diagrammatic point of view. This digression will emphasize an important difference between the generally expected large order behavior of perturbative series in most renormalizable models and the behavior of the above BEC specific series.

---

[2] Remark that in the original calculation[10] corresponding to take $\eta = 0$ in Eq. (3.14), this ambiguity problem has been consistently solved simply by using dimensional regularization (see Appendix A for details): in contrast, the rather subtle point is that when $\eta \neq 0$ in Eq. (3.14) it appears at first perfectly consistent to start with the p integration. Nevertheless, this does not give the correct result, independently of whether one uses dimensional regularization or not, until one correctly identifies what the actual perturbative series in $\delta u/\eta$ should be, as explained above.

In field theory one has to face the problem of the perturbative series being often only an asymptotic (non-convergent) series which, in most cases, is due to factorial growing perturbative coefficients at large orders. If the coefficients are of the same sign, order by order, those series are not even Borel summable [39, 40]. In practice, this means that the perturbative expansion alone does not define uniquely the physical quantities being expanded, so that the series has to be complemented by intrinsically nonperturbative contributions, containing typically terms with an exponential dependence in the (inverse) expansion parameter [40]. This is problematic because, apart from the special case of exactly solvable/integrable models, in most theories those nonperturbative terms are at best known only on phenomenological grounds. However, to investigate the large order behavior of the perturbative series (and therefore guess at least the form of nonperturbative missing contributions), it is often sufficient to consider a class of approximated graphs, expected (and proved in some specific models) to give the dominant contributions to the perturbative coefficients at large order. In dimension $d = 2, 3$ and 4 renormalizable theories, such dominant graphs are typically given by the next-to-leading term in a $1/N$ expansion, where, roughly speaking, the matter fields are in a N-vector representation, and it is sufficient to consider the asymptotic behavior in the bubble $(1/N)$ approximation of the relevant Green functions. For instance, in a theory with a renormalized coupling one obtains, after renormalization, a scale-dependent running coupling. A very sketchy Green's function calculation in the above approximation involves (after renormalization) typical momentum integrals of the form

$$\int dq F(q^2) g(M) \left[1 - \beta_0 g(M) \ln \frac{q^2}{M^2}\right]^{-1} , \tag{3.22}$$

where $F(q^2)$ is model-dependent and characteristic of the Green's function considered, $g(M)$ is the running coupling, β_0 is the first order renormalization group (RG) β-function coefficient: $d\, g(M)/d \ln M \equiv \beta_0 g^2(M) + \cdots$, and M is an arbitrary renormalization scale. When formally expanding Eq. (3.22) in a perturbative series in g, one gets integrals of the form

$$\sum_p g^{(p+1)}(M) (\beta_0)^p \int_0^\infty dq^2 F(q^2) \ln^p \left(\frac{q^2}{M^2}\right) , \tag{3.23}$$

which leads to a factorial behavior $p!$ at large p. More precisely, $F(q^2)$ can be expanded in a power series in q^2 $(1/q^2)$ in the infrared (respectively in the ultraviolet), so that Eq. (3.23) gives series of the form [40] $\sim g^{(p+1)}(-\beta_0)^p\ p!$ or $\sim g^{(p+1)}(\beta_0)^p\ p!$ for large p, respectively, for the infrared and ultraviolet behavior. Considering for example an asymptotically free theory, *i.e.* with $\beta_0 < 0$, one obtains a non sign-alternated series thus non-Borel summable, as far as the infrared behavior is concerned. This fact reflects the important infrared sensitivity of such theories.

Now, a drastic difference between the previous illustration of theories with a renormalized coupling and the effective BEC ϕ^4 model in three dimensions considered here, is that for the latter only the mass is renormalized, so that the coupling is finite and dimensionful, as pointed out previously. From this, and following the above line of reasoning, one expects that the relevant BEC T_c perturbative series coefficients at large orders do not display any factorial behavior. Therefore, a more convergent series should appear, as is confirmed for instance by the form of the exact large-N perturbative series in Eqs. (3.13), (3.21), whose coefficients appear clearly not very different from those of a geometric series. Also, from the above general considerations, a similar behavior of the series is expected as well for arbitrary N. Thus an interesting question is whether one could obtain from such large order behavior estimates a sensible approximation of the exact series in $\delta u/\eta$, that would be relevant within the LDE method.

Let us therefore investigate some analytically simpler but physically motivated approximations (expected to be asymptotically dominant) of the large order behavior of the power series in $\delta u/\eta$, as generated from Eq. (3.16). $B(k, \eta)$ behaves as

$$B(k, \eta^*) \sim \begin{cases} \frac{1}{8\pi}\ \frac{1}{\eta^*}(1 - \frac{k^2}{12(\eta^*)^2} + \cdots), & (k \ll \eta^*) \\ \\ \frac{1}{8\pi}\ (\frac{\pi}{k} - \frac{4\eta^*}{k^2} + \cdots), & (k \gg \eta^*) \end{cases} \tag{3.24}$$

for the IR ($k \ll \eta^*$) and UV ($k \gg \eta^*$) limits, respectively. This means that the deep IR behavior of the series should be essentially given by a k-independent term, $[1 + \delta u N/(48\pi\eta^*)]^{-1}$, replacing the corresponding bracket in Eq. (3.14). Retaining only this simplest IR behavior, the remaining integral over k becomes straightforward and accordingly we

obtain[3] the relevant IR approximated series as a simple geometric series

$$\langle\phi^2\rangle_{IR}^{(\delta)} = -\frac{N\eta^*}{4\pi} - \frac{\delta u N}{24\pi\eta^*}\left[1+\frac{\delta u N}{48\pi\eta^*}\right]^{-1}\left(-\frac{2\eta^*}{4\pi}+\frac{\eta^*}{4\pi}\right) - \frac{\delta u N}{96\pi^2} = -\frac{N\eta^*}{4\pi} + \frac{\delta u N}{96\pi^2}\left[\left(1+\frac{\delta u N}{48\pi\eta^*}\right)^{-1} - 1\right], \quad (3.25)$$

where the first order term, independent of η, has been explicitly subtracted from the naive integral result Eq. (3.16) for consistency, as discussed in detail in the previous Subsec. III.B (note that the purpose of the last parenthesis in the first equality in Eq. (3.25) is to retain, for clarity, the separate contributions of the two propagator terms in Eq. (3.16)). Note also that Eq. (3.16) is UV finite, so that the result Eq. (3.25) is independent of the integration method used, so that either dimensional regularization or another integration method leads to the same result.

Similarly, we can still integrate Eq. (3.14) exactly when taking the UV limit of the propagator, $B(k,\eta^*) \sim (8k)^{-1}$ from Eq. (3.24). One obtains

$$\langle\phi^2\rangle_{UV}^{(\delta)} = -\frac{N\eta^*}{4\pi} + \left(\frac{N\eta^*}{2\pi^3}\right)\left[\pi\, y\left(7+4\,y^2\right) - 8\,\ln(2)\left(1+y^2\right) - 6\,\ln y\right]\left(1+5\,y^2+4\,y^4\right)^{-1} - \frac{\delta u N}{(96\pi^2)}, \quad (3.26)$$

where $y \equiv 48\,\eta^*/(N\,\delta\,u)$. When performing the p integration first, all integrals are UV finite in $d=3$ and again the $\eta \neq 0$ mass explicitly regularizes the IR divergences. Note for instance that in both, Eqs. (3.25) and (3.26), the $1/\eta^*$ and η^* from the first and second integrals respectively, cancel out: this is completely analogous to the cancellation in the original calculation [10], in dimensional regularization with no IR cutoff mass, of the pole $1/(d-3)$ (see Appendix A for details).

Next, remark that by taking the $\eta \to 0$ limit of expression (3.25) or (3.26), one recovers the correct $1/N$ exact result Eq. (A11). In other words, we see here that the massless limit $\eta \to 0$ of the LDE series consistently reproduces the exact large-N result, which is expected since the LDE for $\delta \neq 1$ plays the role of an infrared regulator. But this check is important as regards the question of the possible convergence of the LDE series to the exact result, once a non-trivial optimization of the LDE series, with respect to the arbitrary remaining mass parameter η, will be performed, to be examined in the next section.

With this aim, it is instructive to re-expand, in a power series of $\delta u/\eta^*$, the above two different IR and UV approximations for $\Delta\langle\phi^2\rangle^{(\delta)}$. First, taking the IR limit Eq. (3.25) gives the geometric series in $\delta u/\eta^*$:

$$\langle\phi^2\rangle_{IR}^{(k)} = -\frac{N\eta^*}{4\pi} + \frac{\delta u\, N}{3}\sum_{i=1}^{k} G_i\left(-\frac{\delta u\, N}{6\eta^*}\right)^i \quad (3.27)$$

where $G_i \equiv [(64\pi^2)(8\pi)^i]^{-1}$. Numerically, the first five G_i coefficients are $G_1 = 6.2991\times10^{-5}$, $G_2 = 2.5063\times10^{-6}$, $G_3 = 9.9724\times10^{-8}$, $G_4 = 3.9679\times10^{-9}$ and $G_5 = 1.5788\times10^{-10}$, which are interesting to compare with the corresponding exact coefficients in Eq. (3.21). One can see that the first low order coefficients of Eqs. (3.27) and (3.21) are of very similar magnitudes, and we have further checked that significant departures (*i.e.* about an order of magnitude or more) between the IR-approximated and exact large-N perturbative coefficients only occur at rather large, greater than $\mathcal{O}(\delta^{15})$, orders. In other words, one expects from this comparison the IR-approximated series, which has a convenient and simpler geometric form, to be a very good approximation of the exact large-N series. This is a strong indication that the detailed non-asymptotic (infrared) behavior of the scalar propagator should play essentially no role, as could be physically expected on general grounds, and as will be fully confirmed by our numerical investigation below.

The same expansion for the UV limit (3.26) reads similarly

$$\langle\phi^2\rangle_{UV}^{(\delta)} = -\frac{N\eta^*}{4\pi} + \frac{\delta\, uN}{3}\left[-1.7465\times10^{-4}\left(\frac{\delta u}{3\eta^*}\right) + 2.4737\times10^{-5}\left(\frac{\delta u}{3\eta^*}\right)^2 + \cdots\right]. \quad (3.28)$$

where one can see in contrast that the coefficients are already quite different from the exact series Eq. (3.21) at low order, so that we may expect the asymptotic UV limit of the propagator to give a less sensible approximation than

[3] Note that, in close analogy with Eqs. (3.22), (3.23), we only approximate the non-trivial resummed propagator $B(k,\eta^*)$ according to Eq. (3.24), and keep the exact k,η^* dependence of the remaining integrand.

the IR one. For completeness it is useful to consider alternatively the direct evaluation of Eq. (3.14) (*i.e.* not as a perturbation series in $\delta u/\eta$). Taking thus the exact expression for $B(k,\eta^*)$ instead of its simpler IR or UV limits, the k-integration can be performed only numerically (note that it is still IR and UV finite in $d=3$). Those (numerical) results for the reference value $u=1$ and as function of η^* are illustrated in Fig. 2. As one can see, both the IR and UV approximations, as given in Eq. (3.24), have a behavior that is somewhat different from the exact function Eq. (3.14) for very small η^*, although all expressions correctly give the exact result at $\eta^*=0$. However, though it is not visible on Fig.2, the IR and UV approximations appear to be very good approximations of the exact function for larger $\eta^* \sim \mathcal{O}(1)$, that is in the range where their respective perturbative expansion forms start to be valid.

To summarize this subsection, introducing an IR regulator mass $\eta \neq 0$ as is done from the LDE procedure, together with the deep IR limit of the propagator, Eq. (3.24) in Eq. (3.14) leads to perturbative series that are very close to the exact large-N one in (3.21). The only subtlety when implementing the LDE within the convenient resummed large-N closed form Eq. (3.14), is to remind that one should be careful in exchanging the perturbative series summation with integration, since the resulting integral, Eq. (3.14), is not (absolutely) UV convergent. The consequence is that, *e.g.*, the $\eta^* \to 0$ limit of expression (3.16) does not commute with taking the limit $\eta^* \to 0$ *before* performing any integration, *i.e.* as is done in the original large-N calculation (see Appendix A). This may be considered as a reminiscence of the infrared sensitivity of the theory, even if it is not as severe as the above mentioned models with a running coupling, leading to divergent series with factorial growing perturbative coefficients.

IV. LARGE-N OPTIMIZATION, RESUMMATION AND CONVERGENCE PROPERTIES

As discussed in the introduction, the study of LDE convergence properties in the BEC problem is much more complicated than in the pure anharmonic oscillator case [25, 26, 27, 28]. In principle, both models are described by a scalar ϕ^4 model in one and three dimensions but in the BEC case, the model is used to study a phase transition. However, if the LDE works, one expects that reasonable numerical results should be obtained, converging to the "exact" large-N result, $c_1 = 8\pi/[3\zeta(3/2)^{4/3}] \simeq 2.328$, evaluated in Ref. [10]. Before proceeding, it is useful to point out an essential aspect and potential difficulty of the purely perturbative expansions, Eq. (3.21), or similarly Eq. (3.27). Note that these are *inverse* (alternated) series in the mass parameter η, thus with an a priory finite convergence radius η_c^{-1} (i.e. for $u=1$ these series are (absolutely) convergent only for $|\eta| > \eta_c$) when considered as series for complex values of the arbitrary mass parameter η. But, as discussed above, ultimately the exact result is expected to be recovered for $\eta \to 0$. This situation is not much different from the anharmonic oscillator case, where typically the energy levels have perturbative expansions in powers of λ/m^3 (λ being the coupling and m the mass) with moreover factorially growing coefficients at large perturbative orders, but where nevertheless the LDE converges [25, 26, 27, 28] to the exact result, thanks to an appropriate rescaling of the mass parameter that is consistent with the PMS optimized solutions. We will examine here how the LDE procedure followed by the standard PMS optimization, Eq. (2.2), manage in fact to avoid this $\eta \to 0$ potential problem with the basic perturbation series, which is one of the main results of the present paper. This is where the infrared approximation is a useful guide: while its perturbative form Eq. (3.27) exhibits just the same feature as the exact series, Eq. (3.21), the former geometric series is known to all orders, and obviously its $\eta \to 0$ limit is perfectly well-defined and gives the correct exact result, as can be seen by going back to its original form Eq. (3.25) discussed in Sec. III.C. But no such resummation is a priory known for the relevant non-trivial $N=2$ series, where only the first few perturbative orders in u/η are known and thus only the latter information can be used to define the LDE procedure.

Thus, before considering the LDE of the actual BEC series, it appears very instructive to first examine the same LDE procedure performed on a simpler model which shares many similarities with the relevant BEC problem. We will see that the example below illustrates very well the basic reasons for the success (or eventually failure) of the LDE followed by the PMS optimization method in the general case, beyond the specific BEC problem considered in this paper.

A. A simple example of the LDE-PMS convergence

Let us examine the properties of the LDE and subsequent PMS optimization in a general case by considering the following function which admits a simple alternated geometric series expansion:

$$\Phi(x) = -\frac{1}{x} - \frac{x}{(1+x)} = -\frac{1}{x} + \sum_{n=1}^{\infty} (-x)^n \tag{4.1}$$

which expansion form is almost like our IR geometric series Eq. (3.27), for $u = 1$ and $x \equiv 1/\eta^*$, apart from overall different normalizations (compare *e.g.* with Eq. (3.21) or (3.27)). Clearly, the exact expression in Eq. (4.1) tends to -1 for $x \to \infty$, thus the goal is to examine whether the LDE procedure followed by the standard PMS optimization, which only uses the series expansion form in Eq. (4.1) at successive perturbative orders, is able to reach such a result and in which way. To make contact with the LDE series we consider the series in Eq. (4.1) with $x \equiv u\delta/\eta^*$ (except in the $-1/x$ term on the right-hand side of Eq. (4.1) where we take $x \equiv 1/\eta^*$), followed by an expansion in power series of δ in which one takes $\delta \to 1$. The result of this LDE at arbitrary order k can be expressed entirely analytically in this case (see also Appendix B)[4]:

$$\Phi(x \equiv u/\eta)^{(k)} = -\frac{1}{x}\sqrt{\pi}\frac{(-1)^k}{\Gamma[1/2-k]\Gamma[1+k]} + \sum_{n=1}^{k}(-x)^n \frac{\Gamma[1-n/2+k]}{\Gamma[1-n+k]\Gamma[1+n/2]} \tag{4.2}$$

and the PMS optimization performed order by order (up to order $k = 10$) is shown in Table I. From this table, we can draw several important observations:

i) Applying the PMS optimization condition Eq. (2.2) to $\Phi(x)$ generates complex $\bar{\eta}$ solutions. In addition, all solutions can be arranged into families which span the complex plane. In general, a new family arises at even orders and this is signaled by a first member which lies in the real axis. This pattern was also found in the anharmonic oscillator applications [28] and in the finite N applications to the BEC case [18].

ii) Despite the fact that the (naive) expansion at arbitrary finite order has a finite convergence radius $|x| < 1$ (namely, the LDE at order k only uses the information of the right-hand side of Eq. (4.1), where the series is absolutely convergent for $|x| < 1$), the LDE-PMS procedure clearly converges to the right result for $x \to \infty$ (equivalently $\eta \to 0$) and the convergence is quite rapid in this case.

iii) Though most of the PMS solutions do converge to the correct $x \to \infty$ result, there is a family of real solutions, $S0$, that clearly converges to a different result (~ 2).

iv) Some of the (complex) solutions converge more rapidly than others. In particular, at order 3 one of the solutions is already very close to the exact result, and also one of the two real solutions that does converge to the exact result, which appears only at odd LDE orders, is not the best one. Note also that it is the real part which converges to the right result. However, to obtain those results one must consider all, real and complex, $\bar{\eta}$ values. In fact, the imaginary parts of the complex optimized values $\bar{\eta}$ play an essential role and for instance suppressing even a small imaginary part results in a completely wrong and unstable result for the optimized series. As we shall investigate in more detail below, this is because, for convergence of the series, it is the value of $|x|$ (respectively $|\eta|^{-1}$) which is relevant.

We shall now investigate in more details the basic reasons for the main LDE convergence results ii) above. First, note that in Eq. (4.1) we added an extra term $1/x \sim \eta^*$, since it vanishes for $x \to \infty$. In the relevant BEC case, as already discussed in the previous Section, this term has a very clear physical interpretation, as it corresponds to the tadpole graph. In the present case it may be considered only as a mathematical trick, which plays an important role for convergence. Indeed, when suppressing this extra linear "mass" term, one finds for the LDE-PMS in place of the results shown in Table I: -0.5625 and $-0.6574 \pm 0.153I$ *e.g.* at LDE orders $k = 2$ and $k = 3$ respectively; and at order $k = 10$ the best solution is $-0.97208 \pm 0.285I$ while other solutions are still about 20% away from the exact result. Thus, the additional linear term clearly increases substantially the speed of convergence. First, it is clear that non-trivial PMS solutions already start at order 1, while they start only at order 2 when suppressing this term. But this is not the main reason for this faster convergence. Remark that at very large order, say $k \sim 100$, the numerical accuracy from both procedures (*i.e.* with or without the additional linear term) tend to become essentially equivalent (except that the incorrect solution ~ 2, see iii) above, is absent in the procedure with the linear term suppressed). However, it is evidently crucial to have a procedure such that the very first few LDE orders give already reasonably

[4] Note a slight difference in Eq. (4.2) with respect to Eq. (B2) in Appendix B, namely the Gamma function ratio $\Gamma[-n/2+k]/\Gamma[-n+k]$ in place of $\Gamma[1-n/2+k]/\Gamma[1-n+k]$ appearing in Eq. (B2), due to the fact that Eq. (4.1) does not have the extra factor of $u\delta$ in front of the series. Because of this, non-trivial PMS solutions $d\Phi(x)^{(k)}/dx = 0$ of Eq. (4.2) start already at LDE order $k = 1$, see Table 1. But apart from that, this difference only affects in very minor ways the qualitative behavior discussed below, in particular the large LDE order behavior of the simple series (4.2) with respect to the corresponding actual BEC series.

reliable results, and also to gain an order in the PMS solution, when we will consider the relevant $N = 2$ BEC series for which only the first few perturbative orders are known. The essential role of the linear term is easily understood when expanding the (exact) result in Eq. (4.1) for large x:

$$\Phi(x) = -\frac{1}{x} - \frac{x}{(1+x)} = -\frac{1}{x} - \left(1 + \frac{1}{x}\right)^{-1} = -1 + \mathcal{O}(1/x^2) \tag{4.3}$$

such that for $x \to \infty$ ($\eta \to 0$) the first order $\mathcal{O}(1/x)$ term cancels out. Now what happens is that this cancellation remains after introducing the LDE procedure, thus leading to a faster LDE-PMS convergence, see remarks ii) above, even though the LDE modifies the structure of the perturbative expansion and, as already mentioned, only uses the perturbative information from Eq. (4.1). This can be understood on basic grounds when considering the large k behavior of expression (4.2):

$$\Phi(x \equiv u/\eta)^{(k)} \underset{k \to \infty}{\sim} -\frac{1}{x\, k^{1/2}\, \Gamma[1/2]} + \sum_{n=1}^{k} \frac{(-x)^n\, k^{n/2}}{\Gamma[1+n/2]} \sim -\frac{1}{x\, k^{1/2} \Gamma[1/2]} + \exp(x^2 k)\, Erfc(x k^{1/2}) - 1 \tag{4.4}$$

where $Erfc(x)$ is the standard error function [41], and this large order behavior in (4.4) is obtained after some algebra by using standard properties of the Gamma functions (see also Appendix B). Furthermore, it appears that this large k behavior of Eq. (4.4) exhibiting the scaling $k^{1/2}$ is rapidly reached: for instance the difference between $(-1)^k/\Gamma[1/2-k]/\Gamma[k+1]$ in Eq. (4.2) and $k^{-1/2}/\pi$ in Eq. (4.4) is already $< 4\%$ for $k \geq 3$. Analyzing thus from Eq. (4.4) the large k behavior, one can derive by using the asymptotic expansion of $Erfc(x)$ for the relevant limit $x \to \infty$: $\exp(x^2)\, Erfc(x) \sim 1/(\sqrt{\pi}x)\, [1 + \mathcal{O}(1/x^2)]$ (see also Eq. (B5) in Appendix B), that the first order term $\mathcal{O}(1/x/k^{1/2})$ compensates exactly the linear term, giving in Eq. (4.4) $\Phi(x) \sim -1 + \mathcal{O}(1/x^2/k)$, while omitting the linear term gives instead: $\Phi(x) \sim -1 + \mathcal{O}(1/x/k^{1/2})$. Though the latter properties result from taking the somewhat extreme limit $k \to \infty$, what is quite remarkable is that this behavior is already well observed at very low orders, as the above comparison of numerical PMS optimization in Table I illustrates.

More generally, one can also understand from Eq. (4.4) the main transformation operated by the LDE on the original series: while the latter had a finite convergence radius, for $|\eta| > 1$, the LDE provides an extra damping factor $1/\Gamma[1+n/2]$ which allows to safely reach larger $|x|$ values (equivalently smaller $|\eta|$ values) from the new perturbative series, so that eventually the relevant limit $\eta \to 0$ may be approached. Indeed in practice, namely at finite k orders, all of the PMS solutions $\bar{\eta}$ of Eq. (2.2) corresponding to Table I (except the ones in the first column corresponding to the incorrect solution, as will be discussed below) tend to have smaller and smaller $|\bar{\eta}|$ values (though rather slowly decreasing) as k is increased.

A last remark on the LDE behavior of the simple example (4.1) concerns the occurrence of the incorrect PMS solution, as indicated in iii) above. Clearly, this results directly from the presence of the additional linear term: in absence of the latter, these extra solutions disappear from the LDE-PMS at any orders. Actually, these are reminiscent from the fact that Eq. (4.1) (before LDE is performed), has another extremum at $x = -1/2$ (*i.e.* $\eta = -2$). In the most general case where one would have no a priory idea *e.g.* on the sign of the correct solution, this feature may be considered as a drawback of our procedure. But in fact, it is easy to get rid of this incorrect solution, simply because one knows that the solution we seek should be for $\eta \to 0$. In contrast, the PMS optimized values at successive LDE orders k corresponding to this extra solution are always such that $|\bar{\eta}|$ is maximal, with respect to all other solutions. Furthermore, these $|\bar{\eta}|$ values do not exhibit the expected trend towards smaller and smaller values: on the contrary, the corresponding $|\eta|$ value is (rather slowly) increasing as k is increased.

The important point is that, as we will see below, all of the above properties will be exhibited similarly by the more complicated BEC series and are, therefore, a very useful guideline. In particular, the cancellation due to the additional linear term as above observed, the behavior with the LDE order k of the PMS solutions, including the behavior of the incorrect PMS solution, all occur similarly in the more complicated cases of the actual BEC LDE series, with an expected much faster LDE convergence. These are important remarks concerning the LDE applications since, as already emphasized, the difference between our original applications Refs. [17, 18] and the one performed in Ref. [23] amounts to the fact that the latter authors optimize $\Delta\langle\phi^2\rangle^{(\delta)}$ in Eq. (1.9) which differs from $\langle\phi^2\rangle^{(\delta)}$ by an equivalent linear term.

In the next subsections, we switch to the study of the LDE performed on the actual BEC series in the large-N limit. With this purpose we will consider $\langle\phi^2\rangle_u^{(\delta)}$ as given by the closed form series, Eq. (3.21), and alternatively also its infrared approximation form, Eq. (3.27). These two quantities will be again optimized with the standard PMS criterion, Eq. (2.2). For completeness we also show, with one example, how the alternative Fastest Apparent Convergence (FAC) method, Eq. (2.4), generates similar results. We then present in Sec. IV.C a way to further

rearrange the LDE series, by fully exploiting the above explained behavior of the PMS optimized solutions, which eventually accelerates further the convergence due to the fact that it can recover directly the large LDE order behavior and consequent good $\eta \to 0$ properties of the infrared approximation, with the advantage of being applicable in a general case to more arbitrary series. This technique is then used to treat both the complete closed form and the infrared approximation of $\langle\phi^2\rangle_u^{(\delta)}$, as introduced respectively in Secs. III.B and III.C. For comparison purposes an alternative resummation procedure, based on Padé approximants [42], is also studied in Sec. IV.D. Finally, we analyze all results to conclude in Sec IV.E about the convergence structure of the LDE method.

B. Standard optimization

In order to perform a numerical analysis of the optimized solutions for $\langle\phi^2\rangle_u^{(k)}$ one first expands Eq. (3.13) to the desired order in δ. As usual, one then sets $\delta = 1$ before optimizing. This is the LDE part of the procedure. It can be performed either by explicit order by order expansion, or equivalently more formally following the general structure of the LDE expansion at arbitrary order k as presented in Appendix B, leading to the result Eq. (B2). Like the simple geometric series considered above, Eq. (4.1), the equation for $\langle\phi^2\rangle_u^{(k)}$ is basically a series in powers of $(\delta u)^k/\eta^{(k-1)}$, so that the PMS and Fastest Apparent Convergence procedures will also generate algebraic equations of order k whose mathematically acceptable roots form a set of optima $\bar{\eta}$ values.

Applying the PMS condition, Eq. (2.2), to $\langle\phi^2\rangle_u^{(k)}$,

$$\frac{d\langle\phi^2\rangle_u^{(k)}}{d\eta}\Big|_{\bar{\eta},\delta=1} = 0 \; , \tag{4.5}$$

or the Fastest Apparent Convergence criterion, $\langle\phi^2\rangle_u^{(k)} - \langle\phi^2\rangle_u^{(k-1)} = 0$, computed at $\delta = 1$ (which is again analogous of taking the k-th coefficient in Eq. (2.3), with $\Phi^{(k)} = \langle\phi^2\rangle_u^{(k)}$, equal to zero) generates the optimal results. Table II lists, to order-δ^{20} all families obtained by applying the PMS optimization to the standard closed form expansion given by Eq. (3.21). For completeness we compare, in Table III, results generated with the PMS optimization and the Fastest Apparent Convergence procedures for the same quantity. This table clearly shows that both optimization criteria generate compatible solutions that seem to converge to identical results. We advance that this pattern was also observed in all remaining cases considered in this work, so we shall consider only the PMS optimization, Eq. (4.5), from now on. In addition, we can get more insight by considering our infrared approximated geometric series, Eq. (3.27), which has simple exact coefficients known to all orders. By applying the standard PMS, Eq. (4.5), to this simpler equation one obtains the results shown in Table IV. This table has exactly the same characteristics as Table II except for the positive real part numerical values, that are much closer to the exact large-N value $c_1 \simeq 2.32847$.

Let us try to examine at this stage the (eventual) convergence structure of the LDE as applied to the large-N limit series, namely the results presented in Tables II-III and IV. In both cases the family structure is very similar to the one found for the simple geometric series example in the previous subsection, as well as in the studies that have proven the LDE convergence in the anharmonic oscillator [28]. For instance, we also see in the present case the appearance of a new family at even orders, such that all of them start with a real solution and become complex at the next order, the exception being $F0$ which has only negative real solutions and $F4$ which has only positive real solutions. As mentioned before, the complex parts arise as a consequence of solving the polynomial equations generated during the optimization procedure and are mathematically acceptable. We refrain from trying to attach any physical significance to the complex part of the optima c_1 values and instead of considering only completely real solutions we take the optimized $\mathrm{Re}(c_1)$ as the relevant quantity for the evaluation of T_c, which is a strictly real quantity. Also, in the geometric series application above, we saw that only the real parts of the optimal solutions converge to the expected real value when $x \to \infty$. Considering all complex solutions has also the advantage of giving a prediction at any order. Further, we note that all families whose real parts are positive start with values close to ~ 2.0 and then seem to follow similar patterns as the perturbative order increases. In contrast, considering $F0$ would bring important qualitative changes regarding the critical temperature shift in relation to the ideal gas value, $\Delta T_c = T_c - T_0$, since the sign of this quantity has also been a source of controversy [9] for some time until recently, when most works started to predict positive values for the critical temperature shift. It appears clearly that $F0$ is just the equivalent of the $S0$ (wrong) solution discussed in the simplest geometric series case, which was eliminated because it does not correspond to the $\eta \to 0$ expected behavior. As we will see below, the same criteria allows to eliminate this solution without ambiguity. Pushing further to much higher orders we obtain for the exact $1/N$ series case Eq. (3.21), e.g. at LDE order 100, that most of the positive roots give a solution whose (real part) is ~ 2.2, as well as a few solutions which are far apart reasonable values, which we assume only reflect the numerical limitation of the problem at hand. Indeed, to

obtain those results the numerical procedure involves first to numerically solve the one dimensional integrals related to the J_i coefficients in Eq. (3.21). As emphasized, this has been done with great care with the maximum precision allowed by MATHEMATICA [38] and/or Maple. Yet, one cannot expect the results to be completely stable once the LDE is carried out to very high orders. Though the integration in Eq. (3.18) may be in principle done to arbitrary accuracy, the limitation comes about later in the process of finding the roots of high order polynomial equations, which is a notoriously unstable numerical problem in general. So it is rather the optimization procedure, as implied by the LDE/PMS which is to be carried out numerically, which appears sensitive to numerical accuracy at very high orders. Nevertheless from our analysis all results performed with MATHEMATICA appear under very good control, say until a LDE order of about ~ 50. It looks that all (stable) families in Table II will (slowly) converge, at very high orders, to approximately the same values, in a way again similar to what was observed in the simple geometric series example above discussed in Sec. IV.A and in the anharmonic oscillator case [28]. However, it appears that these PMS optimized solutions in Table II rather converge to a value of about ~ 2.2, *i.e.* close to but not equal to the exact large-N result $c_1 \simeq 2.328$. The reason for this slight discrepancy will be understood below.

In contrast, the results in Table IV illustrate how good the IR approximation is, although from a perturbatively inequivalent approach, and indicates that the LDE series in Eq. (3.25) do converge to the correct result. Pushing the LDE to higher orders, we obtain for Eq. (3.27), for instance at order 100, that most of the solutions are very close (within 0.1% error) to the exact result, the closest solution being $2.32834 \pm 0.00132884I$.

In order to explain the convergence properties on more basic grounds, both for the exact $1/N$ or IR approximated series, one first observes that, similarly to the simple example studied in Sec IV.A above, all of the PMS optimization solutions corresponding to Tables II-IV, except for $F0$, have $|\bar{\eta}|$ starting from relatively large values and then (rather slowly) decreasing as the LDE order k is increased, therefore reaching the boarder of the convergence radius of the original $\delta u/\eta$ series. More precisely, the convergence radius of the geometric series in Eq. (3.27) is immediately given by $R^{-1} = 1/(24\pi)$, so that, for $u = 1$, the original u/η series (before LDE is performed) can only converge if $|\bar{\eta}| > 1/(24\pi) \sim 0.013$. [One expects similarly that the exact large-N original series in Eq. (3.21) should have a convergence radius very close to this $1/(24\pi)$ value, as we actually checked numerically by calculating e.g. $R^{-1} = \lim_{i\to\infty} J_{i+1}/J_i$ to sufficiently high order $i \sim 10^3$]. On the other hand, the exact result should be recovered for $\eta = 0$, thus outside the convergence radius of the original perturbative expansion. Nevertheless, just as explained with the simple geometric series in Sec. IV.A above, this is compensated by the fact that the reorganized LDE series to order k, modify perturbative coefficients of order n with an extra damping factor of $1/\Gamma[1 + n/2]$ (see e.g. Eqs. (B2), (B3) in Appendix B). As a result, this modifies the convergence radius so that smaller and smaller values of $|\eta|$ can be reached, which basically explains e.g. the good convergence of the IR series to the right exact result shown in Table IV. Moreover, an important remark in view of the more interesting application to the finite $N = 2$ case, is to realize that most results produced by the families with real positive parts in Tables II-IV give reasonable values already at very low orders $k \sim 2, 3$, being for instance about 10% away from the exact result. We believe this is not at all a coincidence but simply reflects the faster convergence properties of the PMS solution within our prescription, as discussed in details with the simple example of Sec. IV.A, due to the presence of the linear tadpole term, which implied for the simpler geometric series case an exact cancellation for $\eta \to 0$ of the first order term. For the actual IR geometric series the normalization of the tadpole term relative to the series is however completely different, but because $|\bar{\eta}| \to (24\pi)^{-1}$ as the LDE order p increases, one sees immediately that the first term of the expansion of the tadpole term for $|\bar{\eta}| \to (24\pi)^{-1}$ is $-N/(96\pi^2)$, so that a similar cancellation still occurs, rendering again the convergence somewhat faster.

Based on those general convergence properties considerations, we may also introduce a very simple criteria to select among the multiple PMS solutions as illustrated in Tables II-IV: we can consider the PMS solutions with the smallest $|\bar{\eta}|$, yet such that $|\bar{\eta}|$ is still within the convergence radius of the relevant series. Note that this criteria has also the advantage of automatically eliminating the negative $F0$ solution, as it turns out that the latter always corresponds to the largest (and in fact, slowly increasing with k) $|\bar{\eta}|$ values, just like was the case for the simpler example of Sec. IV.A. Indeed, it is interesting to compare again the exact versus IR approximated $1/N$ series when replacing within their respective LDE expansion to order k this exact value of $\eta = R^{-1}$, instead of the PMS optimized $\bar{\eta}$ values. This is illustrated in Table V, where it clearly appears that the IR approximated series behaves in a somewhat better way than the exact series.

Now coming back to the exact large-N series case in trying to better understand the results in Tables II and III, we can alternatively study numerically the exact expression (3.16) directly, that is performing the integration numerically before expanding in u/η series. In contrast with the latter expansion having (before LDE is performed) finite convergence radius as just discussed above, (3.16) is of course defined for arbitrarily small η. The behavior of this expression for $u = 1$ close to $\eta = 0$ is shown in Fig. 2. As one can see, besides the exact result at $\eta = 0$, Eq. (3.16) gets a real minimum ~ 2.06187 for very small $\eta \sim 0.00235745$. Now it appears clearly that all the LDE solutions in Tables II-III are disturbed by the presence of this real minimum very close to $\eta = 0$: namely in the

process of reaching smaller and smaller η values after the LDE-PMS procedure is applied, the PMS optimization solutions of the LDE at successive orders can be "trapped" into the first minimum reached. In contrast, notice on Fig. 2 that the IR approximated series has a similar real minimum but located exactly at $\eta = 0$, therefore it is not surprising that the PMS optimized LDE does converge correctly into this minimum in this case. This explains why the exact large-N series converges to a value slightly different from the exact one, and is accordingly a weak point of the procedure. In view of this it is interesting to briefly compare the latter results with the alternative prescription such that the LDE-PMS procedure is applied on the same series, Eq. (3.21), but omitting the tadpole term linear in η: $-N\eta^*/(4\pi) = \langle\phi^2\rangle_u^{(\delta)} - \Delta\langle\phi^2\rangle_c^{(\delta)}$. This corresponds to extremizing $\Delta\langle\phi^2\rangle_c^{(\delta)}$ directly (see Eq. (1.9)). This is then similar to the recent LDE convergence studies of Braaten and Radescu [23]. Note that in this case, the additional extremum at very small η is removed. By selecting for simple illustration only the best PMS solutions (*i.e.* the ones whose real parts are the closest to the exact $1/N$ result $\sim 2.328..$), we obtain for c_1 the results shown in Table VI. As one can see, the results in this procedure do converge to the right result, however very slowly. On the other hand, one can also realize that the results at lowest orders $k \sim 3-4$, are far away (more than a factor of 2) from the exact result. In fact, one should wait until about $k \sim 50$ to have a reasonably good approximation. (Moreover, we note that may other solutions that are not shown in Table VI start to be very unstable at such high orders, some being several orders of magnitude away from the correct result). So, even if the series without tadpole term ultimately converges to the right result within this LDE prescription, it appears of not much practical use for the non-trivial $N = 2$ case, where we recall that only the first three perturbative coefficients are known at the moment. This is to be contrasted with the results of Tables I-IV, where the fact that the lowest orders are already a good approximation is, as above explained, a consequence of the cancellation of the first order $\mathcal{O}(\eta)$ term, and of the behavior of the PMS solutions as the LDE order k is increased.

We will next discuss a method which fully exploits these scaling properties of the LDE-PMS solution at large orders, and which accordingly allows directly to resum the LDE perturbative series and to eventually further accelerate the LDE convergence, when applied to our BEC problem.

C. Contour Integral Accelerated LDE Resummation Technique (CIRT)

Having performed the usual LDE interpolation, with $\eta^* = \eta\sqrt{1-\delta}$ and $u \to \delta u$, one obtains the physical quantity Φ expanded to order k. This procedure defines a partial sum that may be written as (see Eqs. (3.13) and (3.21))

$$\Phi^{(k)}(\eta^*, \delta u) \equiv \sum_{n=0}^{k} c_n (u\delta)^n [f(\eta^*)]^n \ , \tag{4.6}$$

where $f(\eta^*)$ is a function of η^* whose form depends on the dimensionality of the physical quantity Φ. As we have already emphasized, the use of η^* is just an economical way to take into account the simple $\delta\eta^2$ vertex. Usually, one expands η^* so that all the terms of order $\leq k$ are present and the direct application of the PMS optimization or Fastest Apparent Convergence to this quantity, at $\delta = 1$, defines the standard LDE. On the other hand, one could be tempted to improve a perturbative series for which the highest order term contains $(\delta u)^k$ and then expand η^* obtaining a higher order series. This may seem artificial at first because the contributions of order greater than k would come only from $\delta\eta^2$ insertions not taking into account, at the same order, new contributions which arise from the quartic δu vertex. However, by construction [43] this procedure helps to accelerate convergence as it gives in a more direct and simple way the large LDE order behavior, as studied by the direct "brute force" LDE method in Appendix B. One may consider an all order resummation by observing that, for $\delta \to 1$, the partial LDE series is given formally, from the simple pole residues, as

$$\Phi^{(k)}(\eta, u, \delta \to 1) = \frac{1}{2\pi\, i} \oint d\delta\, \frac{\delta^{-k-1}}{1-\delta}\, \Phi(\eta, u, \delta) \ , \tag{4.7}$$

where the anticlockwise contour encircles the origin. Now, one performs a change of variables (see Ref. [43] for the original application of this procedure) for the relevant $\delta \to 1$ limit,

$$\delta \equiv 1 - v/k \ , \tag{4.8}$$

together with a similarly order-dependent rescaling of the arbitrary mass parameter, $\eta \to \eta\, k^{1/2}$, where the power $1/2$ is simply dictated by the form of the scalar mass interaction term, $\eta^2\phi^2$ in Eq. (2.6). This rescaling of the mass

parameter is of course consistent with what is obtained by a direct study of the large k behavior of the standard LDE, see Appendix B.

For $k \to \infty$ this resummation takes the final form of the replacement

$$\eta^* \to \eta v^{1/2} \ , \tag{4.9}$$

followed by the contour integration

$$\Phi^{(k\to\infty)}(\delta \to 1) = \frac{1}{2\pi i} \oint \frac{dv}{v} \ \exp(v) \Phi(\eta^* \to \eta v^{1/2}) \ , \tag{4.10}$$

where the "weight" $\exp(v)/v$ originates from

$$d\delta \, (1-\delta)^{-1} \to -dv/v \ , \tag{4.11}$$

and

$$\lim_{k\to\infty} (1 - v/k)^{-k-1} = \exp(v) \ , \tag{4.12}$$

while the original contour was deformed to encircle the branch cut $Re(v) < 0$. Here, one is initially dealing with a power series in $(\delta u)[\delta u/\eta^*]^i$ (cf. e.g. Eqs. (3.6), (3.8)) and so, the use of

$$\oint dv \exp(v) \ v^a = 2\pi \, i/\Gamma(-a) \ , \tag{4.13}$$

shows that the main effect of this resummation is to divide the original expansion coefficients at order-$\delta^{(i+1)}$ by terms $\Gamma(1 + i/2) \sim (i/2)!$ for large n. This damping of the perturbative coefficients at large order, as implied by this specific resummation, is fully consistent with what is obtained by a direct "brute force" resummation of the LDE series for large order $k \to \infty$, see e.g. Eqs. (B2), (B3) in Appendix B. But such a damping is rather generic and was exploited recently in the completely different context of asymptotically free models [30] where it was shown to accelerate convergence of the LDE. When applied to the anharmonic oscillator, it is in fact (asymptotically) equivalent to the more direct LDE resummation with an order-dependent rescaling of the arbitrary mass, as employed in some of the Refs. [25] to establish rigorous convergence of the LDE for the oscillator energy levels, that is itself an extension of the order-dependent mapping (ODM) resummation technique (see, Seznec and Zinn-Justin in Ref. [13]). In fact, this procedure can essentially suppress the factorial behavior at large orders of the perturbative coefficients generic in many theories, and convergence may be obtained even for series that are originally not Borel summable [25, 30]. The above contour integral resummation is very convenient since it is algebraically simpler than the direct LDE summation (compare with Appendix B). In the present case, one expects fast convergence since the original series has no factorially divergent coefficients.

Let us start by treating the standard closed form result of this contour integral accelerated resummation technique (CIRT) transforming Eq.(3.21) into

$$\langle \phi^2 \rangle_u^{(k)} = -\frac{N\eta}{4\pi\Gamma(1/2)} + \frac{Nu}{3} \sum_{i=1}^{k} \frac{J_i}{\Gamma(1+i/2)} \left(-\frac{uN}{6\eta} \right)^i \ , \tag{4.14}$$

which clearly displays the coefficients damping. Then, by applying the PMS, Eq. (4.5), one obtains the results displayed in Table VII. This table shows that only the lowest order real parts of the positive families produce reasonable results but the values seem to deteriorate at high orders. Again, one observes that all positive families have similar behavior, starting from values close to ~ 2.000 the values decrease and then start to increase, as exemplified by $F1$. Table VII seems to show that the disturbance due to the presence of the extra minimum of Eq. (3.16): ~ 2.06187 for very small $\eta \sim 0.00235745$, reflected in the data of Table II, get amplified by the CIRT which resums the series. This effect will be further discussed in Sec. IV.E below.

We shall now examine how the all order LDE summation can further improve the convergence of the series. To see that, we consider again the IR behavior (3.25), that is sufficient to grasp the essential features by keeping all results

fully analytical. Applying thus the CIRT method to the simpler geometric IR series, Eqs. (3.25) and (3.27), we obtain the result

$$\langle\phi^2\rangle_u^{(k)} = -\frac{N\eta}{4\pi\Gamma(1/2)} + \frac{Nu}{96\pi^2}\left[\sum_{i=0}^{k}\frac{(-x)^i}{\Gamma(1+i/2)} - 1\right] = -\frac{N\eta}{4\pi\Gamma(1/2)} + \frac{Nu}{96\pi^2}\left[e^{x^2}Erfc(x) - 1\right] \tag{4.15}$$

with $x \equiv N\,u/(48\pi\eta)$ and $Erfc(x) = 1 - Erf(x)$ is the standard error function (see also Appendix B). Next, upon using the well known asymptotic expansion of $Erfc(x)$ for $x \to \infty$ (*i.e.* $\eta \to 0$) [41] (see Eq. (B5) in Appendix B), we can again apply the PMS optimization procedure at given successive orders k. The PMS optimization generates the results shown in Table VIII. Note how the large-N result, $c_1 = 8\pi/[3\zeta(3/2)^{4/3}] \simeq 2.328$ is *exactly* reproduced already at the lowest non-trivial order. Moreover, as one can see from that table, this real solution remains valid at any order in perturbation theory. Thus, the exact large-N result is recovered from this exact CIRT resummation of the LDE, even if we have only used the IR approximation of the propagator. The convergence to the exact $1/N$ result in this alternative LDE implementation is extremely rapid upon using the CIRT. This also indicates that the convergence to the exact result can be independent of the details of the non-asymptotic behavior of the perturbative series coefficients, at least for the large-N quantity here considered.

An important feature of the CIRT-PMS results in Table VIII is that the asymptotic expansion in Eq. (B5) implies that we are now dealing with a series in η/u, instead of the standard perturbative series in u/η, which we started from, as in Eqs. (3.13), (3.21), or (3.27). This is a consequence of the IR approximation, leading to the simple geometric series in u/η, Eq. (3.27), whose all order CIRT form has an exact expression, Eq. (4.15), that can be re-expanded in a η/u series. The reason why the convergence properties of such a series are much better than those of the original series should now be clear in view of the discussion in previous subsections: the original theory is to be recovered in the limit $\eta \to 0$, which is clearly not in the (finite) convergence domain of the original u/η series, while it is automatically inside the convergence domain of the all LDE order resummed series Eq. (4.15). Moreover, another advantage of this reverted series approach is that we may bypass the need of PMS or other similar criteria: clearly the best approximation to the exact result will be simply given by the smallest η values, irrespective of whether it is a solution of a PMS (or similar) criteria.

D. LDE from Padé approximants

For completeness we will also consider in this subsection the results obtained from a completely different resummation of the relevant BEC series, based on the Padé approximant (PA) method [42]. We define, as is standard, a PA $P[n,m]$ as a rational fraction of two polynomials of order n and m respectively in the relevant variable u/η:

$$P[n,m](u/\eta^*) \equiv \frac{\sum_{i=0}^{n} a_i (u/\eta^*)^i}{\sum_{j=0}^{m} b_j (u/\eta^*)^j} \tag{4.16}$$

where the perturbative coefficients a_i and b_j are obtained order by order by expanding Eq. (4.16) up to order $n+m$ and matching the resulting series with the original expansion. We recall that PA are generally useful when a series is known only up to the first few orders, as they can predict sometimes with a very good accuracy the unknown higher orders, and/or give very good resummation results. As far as the BEC series is concerned, our further motivation to consider PA is that it will allow to simply define an alternative (approximated) series in the *inverse* variable η/u, starting from the exact large N (or finite N as well) series Eq. (3.13). As illustrated in previous subsection with the IR approximated series that has an obvious alternative expansion in η/u, since the exact result is recovered for $\eta \to 0$, we shall expect much better convergence properties from such an inverted series, as will be seen below. Note also that the PA method is largely independent of the previous methods, so that it can provide a further consistency cross-check of the numerical results. Another advantage is that the PA technique is immediately applicable as well to the finite N case, to be discussed below in Sec. V. A drawback of the PA method, however, is that they are not uniquely defined, since for a given perturbative expansion of order k one may consider a priory all possible PA with $n+m=k$. In order to thus limit somehow the number of possible PA without introducing much bias in our analysis, we will only consider resulting PA that can be expanded in powers of η/u, for the reasons discussed above, which imposes that $n < m$. To illustrate in the most simple case the power of PA, let us first consider again the IR approximated geometric series Eq. (3.27), but assuming that only the first order term of the u/η series is known: $\langle\phi^2\rangle_{IR} \sim -(N\eta^*)/(4\pi) + (\delta u N)/[(96\pi^2)(8\pi)](-\delta u\, N)/(6\eta^*)$. We could then define an approximation of this series as follows

$$\langle\phi^2\rangle_{IR} \sim -\frac{N\eta^*}{4\pi} + \frac{\delta u N}{96\pi^2}[P[0,1](u/\eta^*) - 1] \tag{4.17}$$

where the PA of order $n+m=1$ is

$$P[0,1](u/\eta) \equiv [b_0 + b_1\delta\, uN/(6\eta)]^{-1}\,, \tag{4.18}$$

and a simple matching of the expansion of (4.17) gives $b_0 = 1$ and $b_1 = 1/(8\pi)$, such that the exact geometric series is in fact recovered, and can be of course expanded in the alternative form of a η/u series. Though this example maybe too simple, we can expect that the more general PA that are constructed below to approximate the more complicated exact series, will have similarly good resummation properties. Typically at order 3 we have to consider $P[1,2]$ and $P[0,3]$. The PA results are shown in Table IX for the large N case. The order k designates in this case the order of the (re)-expansion in LDE power series of the PA, followed again by a standard PMS optimization. Higher orders $k > 5$ are not shown but exhibit a very stable behavior with solutions almost similar to the lowest orders shown. As one can see, the exact result is often reproduced as a PMS solution, which is not so remarkable in the present $1/N$ case, as it simply means that $\eta = 0$ (for which value the PA is well-defined by construction) is a solution when applying the PMS to the PA. Clearly the best PMS solutions, if $\eta \neq 0$, are obtained from the smallest $|\eta| \neq 0$ values. Though it appears clearly that the PA $P[0,3]$ give much better results than the $P[1,2]$, note that the latter give solutions ~ 2.05 and ~ 2.6 that are located not far below and above the exact value. The better $P[0,3]$ results maybe eventually explained by noting that the $P[0,3]$ should have much better resummation properties for $\eta \to 0$, having no numerator term in u/η.

Another advantage of the PA is that one may skip the PMS criteria and simply take the limit $\eta \to 0$ directly, in which case the exact $1/N$ result is reproduced. Of course as concerns the large-N case those results are only a consistency cross-check, since we started from the exact series anyway and thus only managed to define a PA such that its $\eta \to 0$ limit is well-defined, in contrast with the naive u/η series. But the very same PA procedure can be applied to the finite N case to be discussed in the next Section.

E. Brief summary and discussion of the convergence properties

One may now summarize the main features of this detailed large-N investigation so that the finite N application, in the next Section, can be carried out straight away. Regarding the family selection one notes, especially in Tables II and IV, that except for $F0$ all families produce results that converge to approximate similar values at high orders, as in the anharmonic oscillator an geometric series cases. Therefore, choosing consistently $F1$ in all the BEC applications appears to be an appropriate choice since this family is also the only one which allows predictions at any order (*e.g.* in a computation involving only low orders in δ). Again, this is consistent with the observations drawn from the geometric series analysis.

To understand completely the reason for convergence it is particularly convenient to examine the formal expressions of the large LDE order behavior, i.e. for $k \to \infty$, as derived in details in Appendix B. What happens, as already explained in Sec. IV.B, is that when the LDE order is increased, the numerical PMS optimal solutions $|\bar{\eta}|$ tend to be smaller and smaller and thus to reach the boarder of the convergence radius of the original perturbative series. But at the same time, from the study of the asymptotic behavior of the series at large LDE orders we see that the main effect of the rearranged LDE series is to provide an extra damping factor $1/\Gamma[1+n/2]$ as well as a scaling factor $k^{n/2}$ in its order n coefficient. So, after redefining conveniently $\eta \to \tilde{\eta}k^{1/2}$, the *new* optimized $\tilde{\eta}$ values can tend to zero, for which the new LDE-resummed series is now more and more convergent (see *e.g.* Eq. (4.15)) and leads to the correct $\eta \sim 0$ result. However, in the process of reaching smaller and smaller values, it may happen that another non-trivial extremum, if present, is first met, in which case the convergence is disturbed or slowed down by the presence of this other extremum and the $\eta \to 0$ may no longer be reached. This is precisely what happens in the case of the exact $1/N$ series, as illustrated above in Tables II and III, with this problem worsening as the series is resummed, as shown by the results in Table VII, for the CIRT resummation applied to the exact large-N perturbative series. In contrast, by using the IR series approximation the disturbing extremum that now approaches $\eta \neq 0$ is removed and this problem is not present there. Finally, we mention that the recent LDE convergence studies of Braaten and Radescu [23] follow the same lines of the standard LDE calculations performed by us in Sections III.B and IV.B. The major difference being that those authors prefer to extremize $\Delta\langle\phi^2\rangle_c^{(\delta)}$ directly (see Eq. (1.9)). In practice, the difference in between those physical quantities amounts to the tadpole term $-N\eta^*/(4\pi) = \langle\phi^2\rangle_u^{(\delta)} - \Delta\langle\phi^2\rangle_c^{(\delta)}$, that appears in Eqs. (3.13) and (3.21). In the case of the standard LDE-PMS application, like the one shown in Table II, their numerical results

are similar to ours at very large orders, exhibiting ultimately convergence, but do not give a good approximation at the lowest orders. The reason for this faster convergence when the tadpole term is present is the cancellation of the leading terms for $\eta \to 0$ as explained in detail above. Our simple geometric series investigation has also shown the crucial role, regarding convergence, played by this type of linear term. Moreover, these type of loop terms are also at the origin of good convergence properties observed in many other applications [28, 32, 33].

V. THE FINITE N CASE WITH RESUMMATION OF THE LDE

Let us now turn our attention to the finite N results and, especially, to the improvement of the LDE within this limit by using the CIRT resummation method discussed in the previous Section. The insight gained in the detailed large-N study will prove to be very useful to understand the structure of optimized results and to select the appropriate solutions. For arbitrary N, the quantities $\langle\phi^2\rangle_u^{(k)}$ as well as $\delta r_c^{(k)}$ have been evaluated in details, up to order-δ^4, in Ref. [18]. The contributing diagrams evaluated in that reference for the δ perturbative expansion of $\langle\phi^2\rangle_u^{(k)}$ to order-δ^4 are shown in Fig. 3. In Ref. [18] all the integrals appearing in those diagrams were obtained with the type of perturbative calculation discussed in Subsec. III.A with the multidimensional Feynman integrals calculated with VEGAS. Those terms were also later been obtained by Braaten and Radescu [23] in a different way, by reducing the multidimensional integrals to one-dimensional ones in some of the terms of fourth order in δ and, more recently, Kastening in Ref. [44] has also revised those numerical results, obtaining more precise numerical results for the integrals. From the results originally obtained in Ref. [18] and using the corresponding updated, higher precision coefficients evaluated in [44], the terms contributing to $\langle\phi^2\rangle_u^{(k)}$ to order-δ^4, shown in Fig. 3, are given by

$$\begin{aligned}
\langle\phi^2\rangle_u^{(4)} &= -\frac{N\eta^*}{4\pi} - \delta^2\frac{u^2}{\eta^*}\frac{N(N+2)}{18(4\pi)^3}[0.14384] \\
&+ \delta^3\frac{u^3}{(\eta^*)^2}\frac{N}{(4\pi)^6}\frac{\left(16+10N+N^2\right)}{108}[8.06940] + \delta^4\frac{u^4}{\eta^3}\frac{N(N+2)^2}{(18)^2(4\pi)^7}[0.11507] \\
&- \delta^4\frac{u^4}{\eta^3}\frac{N}{(4\pi)^7}\frac{\left(40+32N+8N^2+N^3\right)}{648}[3.12811] - \delta^4\frac{u^4}{\eta^3}\frac{N}{(4\pi)^7}\frac{\left(44+32N+5N^2\right)}{324}[1.71859] \\
&+ \delta^4\frac{u^4}{\eta^3}\frac{N(N+2)^2}{108(4\pi)^7}[0.20821] - \delta^4\frac{u^4}{\eta^3}\frac{N}{(4\pi)^7}\frac{\left(44+32N+5N^2\right)}{324}[2.66746] + \mathcal{O}(\delta^5)\ . \qquad (5.1)
\end{aligned}$$

where, as before, $\eta^* = \eta\sqrt{1-\delta}$ must be expanded accordingly to take into account all contributions shown in Fig. 3. The symmetry factors appearing in Eq. (5.1) can be found e.g. in [45]. The symmetry coefficients clearly show that this perturbative expansion is valid for any N which means that, up to order-δ^4, the large-N results Eqs. (3.13) and (3.21) may be recovered, within numerical error bars of about 2%. This evaluation is easily done by considering u to be of order $1/N$ so that only $(uN)^k$ terms are retained together with the first, u-independent term. Fig. 3 illustrates well how the LDE mixes, at a given order, diagrams which normally appear at different orders in the $1/N$ expansion.

By setting $N = 2$ one then gets the more compact form

$$\langle\phi^2\rangle_u^{(4)} = -\frac{\eta^*}{2\pi} + \delta u\sum_{i=1}^{3} K_i\left(-\frac{\delta u}{\eta^*}\right)^i + \mathcal{O}(\delta^5)\ , \qquad (5.2)$$

where the coefficients are $K_1 = 3.22158\times10^{-5}$, $K_2 = 1.51792\times10^{-6}$, $K_3 = 9.66514\times10^{-8}$. It is worth remarking that the coefficients K_1 and K_2 obtained from the numerical results of Ref. [18] agree with these results, also obtained later by the authors of Refs. [23, 44]. At the same time the K_3 coefficient used here, which was obtained in Refs. [23, 44], differs by about 10% from the one that would come from the results of Ref. [18]. We in principle can trace this difference by the fact that five non-trivial graphs with five loops enter the evaluation of K_3 (see Fig. 3), which require some careful calculation[5].

Then, by applying the standard PMS, Eq. (2.2), to Eq. (5.2) one obtains three families, shown in Table X, in agreement with Ref. [18]. Turning to the CIRT resummation of Eq. (5.2) one proceeds as in the large-N case (see Sec.

[5] We thank B. Kastening for pointing out to us the correct values for the five-loop diagrams and for discussions concerning the difficulties in evaluating them.

IV.C). By applying the CIRT improved in the context of the PMS optimization to Eq. (5.2) one obtains three other families, also shown in Table X. In fact, the previous large-N analysis strongly suggest that also here the first family with positive real parts should be the relevant family concerning our $N = 2$ predictions. Indeed, if we assume that the large order behavior of the actual $N = 2$ series coefficients should not be drastically different from the analogous large-N series, all the fast convergence and scaling properties that were discussed in Sec. IV should be approximately valid also for $N = 2$. Then, the first negative family in Table X is easily eliminated by the same criteria as in the large-N case, because it again always corresponds to the largest $|\bar{\eta}|$ and does not exhibit any trend towards smaller $|\bar{\eta}|$ values as the LDE order k is increased. Similarly, we also notice that the F_1 family in Table X has $\mathrm{Re}(\bar{\eta})$ substantially smaller than F_2, while we expect the exact result to be for $\eta \to 0$. Moreover, due again to the presence of the tadpole term in our procedure, from the analysis in Sec. IV we can expect that our results, though intrinsically limited for $N = 2$ to the first four LDE orders, should be nevertheless already a reasonably good approximation.

A further crosscheck of the consistency of our results without any knowledge of the exact higher order coefficients for the case $N = 2$, is the stability of the result when replacing these unknown perturbative coefficients by a well-defined approximation. This is the result exhibited in Table XI, where the unknown order K_i with $i \geq 4$ were replaced by the corresponding coefficients of the IR approximated series, Eq. (3.27). As one can see, the stability of those results is quite remarkable, and one can even observe the slow convergence of the standard LDE-PMS to the CIRT result.

The physically meaningful real part of our order-δ^4 CIRT improved result $c_1 \simeq 1.19$ can then be compared with the recent Monte Carlo estimates $c_1 = 1.32 \pm 0.02$ and $c_1 = 1.29 \pm 0.05$. Note that the standard order-δ^4 PMS result, $c_1 \simeq 1.53$ is also a satisfactory estimate. We note that the CIRT and ordinary PMS results just bound the Monte Carlo estimates from below and above, respectively.

Finally, in Table XII we show the results for c_1 obtained by Padé approximants (PA), as discussed in the last Section. As expected, at first non trivial LDE order (order 3), only the $1/N$ solution is found from the PA, because only $\eta = 0$ is a PMS optimization solution. As one can see, the non-trivial results at higher orders (5–10) of the LDE expansion in Table XII are nicely consistent with what is independently obtained from the standard LDE and CIRT results shown in Table X. Note however that the PA $P[0, 3]$ are in better consistency than the $P[1, 2]$, which in fact only give result very similar to the ones in the large-N case shown in Table IX.

The contributions to $\delta r_c^{(4)} = -\Sigma_{\rm ren}^{(4)}(0)$, which enter in the derivation of the constant c_2'', Eq. (1.6), have also been explicitly evaluated in Ref. [18] and again we refer the interested reader to that reference for the details and we show below only the final result for the renormalized, scale (M) dependent $\delta r_c^{(4)}$ obtained in that reference:

$$\begin{aligned}
-\delta r_c^{(4)} \;=\; & \Sigma_{\rm ren}^{(4)}(0) = -\delta u \frac{\eta^*}{8\pi}\left(\frac{N+2}{3}\right) - \delta^2 \frac{u^2}{(4\pi)^2}\frac{(N+2)}{18}\left[\ln\left(\frac{M}{\eta^*}\right) - 0.59775\right] \\
& - \delta^3 \frac{u^3}{\eta^*}\frac{(N+2)^2}{108(4\pi)^3}[0.143848] + \delta^3 \frac{u^3}{\eta^*}\frac{\left(16+10N+N^2\right)}{(4\pi)^5 108}[81.076] \\
& + \delta^4 \frac{u^4}{\eta^2}\frac{(N+2)}{6(4\pi)^6}\frac{\left(16+10N+N^2\right)}{108}[8.09927] \\
& - \delta^4 \frac{u^4}{\eta^2}\frac{\left(40+32N+8N^2+N^3\right)}{(4\pi)^6 648}[20.43048] - \delta^4 \frac{u^4}{\eta^2}\frac{\left(44+32N+5N^2\right)}{(4\pi)^6 324}[12.04114] \\
& - \delta^4 \frac{u^4}{\eta^2}\frac{\left(44+32N+5N^2\right)}{(4\pi)^6 324}[17.00434] + \delta^4 \frac{u^4}{\eta^2}\frac{(N+2)^2}{(18)^2(4\pi)^6}[2.8726] + \mathcal{O}(\delta^5)\;, \qquad (5.3)
\end{aligned}$$

which, for $N = 2$, becomes

$$\delta r_c^{(4)} = -\Sigma_{\rm ren}^{(4)}(0) = \delta \frac{u\eta^*}{6\pi} + \delta^2 u^2 A_2\left[\ln\left(\frac{M}{\eta^*}\right) - 0.59775\right] - \delta^3 \frac{u^3}{\eta^*}A_3 + \delta^4 \frac{u^4}{(\eta^*)^2}A_4 + \mathcal{O}(\delta^5)\;, \qquad (5.4)$$

where $A_2 = 1.40724 \times 10^{-3}$, $A_3 = 8.50859 \times 10^{-5}$ and $A_4 = 3.52299 \times 10^{-6}$. The application of the PMS optimization to Eq. (5.4) reproduces the same results as obtained in Ref. [18] which are ~ 101.4, ~ 98.2 and ~ 82.9 from second to fourth order respectively.

At the same time, treating $\delta r_c^{(4)}$ with the CIRT (from Sec. IV.C) one obtains the result[6] $\mathrm{Re}\,[r_c^{(4)}(M = u/3)] = 0.0010034u^2$ which, together with the CIRT improved $\langle\phi^2\rangle_u^{(4)}$ result, and Eq. (1.6), leads to (with errors estimated

[6] Note that the scale $M = u/3$ was originally chosen in the Monte Carlo applications [8].

from the integrations performed in [18] with Vegas) $c_2'' = 84.9 \pm 0.8$ whereas the Monte Carlo result is $c_2'' = 75.7 \pm 0.4$ [8]. To our knowledge, these are the only analytical predictions for this coefficient to the present date. For consistency, note that the optimization of $\delta r_c^{(4)}$, including the selection of solutions, has also been performed according to what was done for $\langle\phi^2\rangle_u^{(\delta)}$.

Note that we have not attempted to examine the infrared behavior of the finite N case since its series is much more complicate than the large-N one. However, our previous large-N investigation shows that the LDE works well, even for the standard series, already when considering only the lowest order terms. Here, only these lowest order terms were computed so that our results, up to order-δ^4, can be considered good estimates even if one knows that the whole procedure may get spoiled at very high orders.

VI. CONCLUSIONS

We have investigated how the LDE followed by a standard PMS optimization performs in the non-trivial case of phase transitions of interacting homogeneous dilute Bose gases described by an effective three dimensional ϕ^4 field theory. This nonperturbative method has been recently employed in Refs. [17, 18] and in Ref. [23] to determine the critical temperature for such a system, giving good numerical results. One advantage is that the formal calculations are performed exactly as in the perturbative case. This means that, at each order, one deals with a very reduced number of contributions which are not selected according to their topology (like the number and type of loops). Therefore, the method is valid for any finite value of N. To handle ultraviolet divergences, the renormalization program is implemented as in the usual perturbative way. Also, an arbitrary mass parameter consistently introduced by the method avoids any potential infrared problems.

The convergence properties, including rigorous proofs, of those nonperturbative methods have been studied in quantum mechanics [25, 26, 27, 28] and more recently in quantum field theory [30]. However, despite the many successes obtained with the LDE in different applications, the convergence study in the BEC case poses new challenges. One of the reasons is that it is difficult to establish simple analytical links between the LDE and other nonperturbative methods at the one-loop level, since those terms do not contribute at the transition point. This could rise the suspicion that the results obtained in Refs. [17, 18], for the realistic $N = 2$ case, are just a numerical coincidence. The exact value for the linear coefficient c_1 which appears in the critical temperature of interacting homogeneous dilute Bose gases is still unknown [9] although much progress has been recently made concerning its determination [14]. Here, our aim was to prove the reliability of the recent LDE results for c_1 and c_2'' [18] through a detailed analysis of the LDE convergence properties.

We have started our convergence study by considering the effective BEC model in the large-N where the results obtained by Baym, Blaizot and Zinn-Justin ($c_1 \simeq 2.328$) [10] can be considered "exact". We have performed the usual perturbative LDE evaluation of $\langle\phi^2\rangle_u^{(\delta)}$ in different ways which allow for numerical accuracy checks. By considering the asymptotic infrared behavior of the propagator we have obtained a simpler series with exact coefficients which allows for a fully analytical analysis. Before tackling the optimization of the BEC series we have investigated how the procedure works considering a simple geometric series. The insight gained during this exercise proved to be very important in understanding the family structure of optimal solutions with regard to convergence properties. Then, the standard series and its infrared limit have been optimized with the PMS criterion, Eq. (2.2), leading to reasonable results in the standard case (see Table II). At the same time, the numerical results produced by the same optimization applied to the infrared series display better convergence properties, as shown in Table IV. This also shows that the optimization procedure is rather sensitive to the actual form of the perturbative expansion series coefficients, in particular at low perturbative orders. Indeed, we emphasize again that including the linear tadpole term in the LDE-PMS procedure is crucial for a faster convergence and to obtain an already very good approximation at low perturbative orders, though both procedures tend to similar results at very high orders.

We have then presented an efficient all order resummation technique, similar to the one used to prove the LDE convergence within quantum field theories at zero temperature [30]. This LDE resummation method takes advantage of contour integration techniques which allows to resum more directly the series and thus to accelerate convergence. Applying this contour integral resummation technique (CIRT) to the exact large-N perturbative LDE series seems however at first to amplify the numerical instabilities generated through numerical optimization. This problem becomes more severe as one moves to higher perturbative orders as shown in Table VII. On the other hand, applying the CIRT to the infrared series *exactly* reproduces the large-N value $c_1 = 2.328$ already at the first non-trivial order. This solution has no complex parts and remains valid as one goes to higher orders while all other families of solutions display good convergence properties having real parts that are numerically very close to the exact value (see Table VIII). In summary, this extensive analysis has shown that, for this type of series, the optimization procedure and convergence rate may be influenced by the actual values of the first few perturbative order coefficients. We have

shown that, for this effective BEC model, the simple infrared series retains all the nonperturbative information and that the LDE, augmented with the CIRT, performs rather well. Finally, we have seen that all families, display a very similar structure and will predict approximately the same values at high perturbative orders. We also have shown how the family which produces negative c_1 values is easily eliminated because it does not correspond to the expected trend towards small $|\eta|$ values of the PMS solution. The very same criteria allows to single out the values generated by the first family of positive solutions, both for the large-N or finite N case. Finally, the results obtained by a different resummation based on Padé approximants, aimed as an alternative to define the relevant $\eta \to 0$ limit from the perturbative series in u/η prior to LDE, appear quite consistent with the latter ones.

More formally, our present study investigated in some detail the large order behavior of the LDE (e.g. in Sec. IV.C with the CIRT method or alternatively in Appendix B), from which we can also point out interesting analogies as well as differences with the LDE convergence properties in quantum mechanics for the anharmonic oscillator[25, 26, 27, 28]. The latter is described by a (one-dimensional) scalar theory with a ϕ^4 interaction term, and as is well-known its energy levels have perturbative expansion coefficients that are factorially growing at large orders[35]. Nevertheless, as already mentioned in Sec. II, the LDE can converge essentially because the PMS optimized solutions behave like a rescaling of the mass parameter with perturbative order which can compensate the factorial behavior at large orders. In contrast, the relevant BEC perturbative series here considered in Sec. III have a finite convergence radius, such that no explicit rescaling of the mass parameter should be necessary in principle for convergence. Nevertheless, what the LDE followed by PMS optimization is performing is to enlarge the original series convergence radius, thus qualitatively similarly in this respect with the oscillator. These properties of the LDE are best exploited by the CIRT more direct resummation method.

The final part of the work was devoted to the realistic finite N case for which only the standard series with coefficients numerically obtained is available. In practice, here only the first low orders contributions could be evaluated and the comparisons performed in the large-N show that VEGAS produces, in this case, accurate coefficients which should not completely spoil the optimization procedure. For consistency with the large-N case we have considered only the real parts of the first family of positive solutions as the relevant ones. Applying the CIRT to this case has improved the recent order-δ^4 results of Ref. [18], generating $c_1 \simeq 1.19$ and $c_2'' \simeq 84.9$, which are about 9% smaller and 11% higher, respectively, than the recent lattice Monte Carlo estimates [14, 15]. In any case one cannot expect to make a definitive analytical prediction, for those coefficients, from a calculation involving only a handful of contributions. Nevertheless, the agreement between our improved analytical LDE results and the recent numerical Monte Carlo results is quite impressive. Moreover, the consistency of our $N = 2$ results as obtained from a different resummation method (Padé approximants) used prior to the LDE procedure is also noticeable. Our results seem to support the fact that, analytically, the leading contributions to ΔT_c for the BEC case studied here can be obtained by resumming typical leading and next to leading $1/N$ type of graphs as in Refs. [11] and [18]. The better LDE numerical values may be due to the mixing of such contributions since in reality, $N = 2$.

In summary, our detailed convergence study together with the improved optimization procedure results show the potential of the LDE to tackle nonperturbative calculations in field theory at critical points. We have explicitly shown how meaningful non perturbative results for the BEC problem can be obtained in a consistent fashion which also works for a general case such as the simple geometric series analyzed in the paper.

Acknowledgments

M.B.P. and R.O.R. were partially supported by Conselho Nacional de Desenvolvimento Científico e Tecnológico (CNPq-Brazil). M.B.P. also acknowledges the LPMT in Montpellier for a CNRS *Poste Rose* grant. The authors thank Gilbert Moultaka for discussions related to Sec. IV.

APPENDIX A: REVIEW OF THE ORIGINAL LARGE-N CALCULATION.

Let us briefly recall how the exact large-N derivation of c_1 was performed in the original calculation, Ref. [10], in order to exhibit the differences with the LDE (exact or approximated) evaluation as performed in Sec. III. Considering the original theory described by Eq.(1.8) at the critical point, the Hugenholtz-Pines (HP) theorem imposes [7, 14] $r_c = -\Sigma(0)$, where $\Sigma(0)$ represents the field self-energy with zero external momentum. Then, one has a massless propagator and the appearance of IR divergences has to be carefully dealt with. In Ref. [10], after applying the HP theorem, the relevant expression for $\Delta\langle\phi^2\rangle$ reads

$$\Delta\langle\phi^2\rangle = \langle\phi^2\rangle_u - \langle\phi^2\rangle_0 = N\int \frac{d^3p}{(2\pi)^3}\left[\frac{1}{p^2+\Sigma(p)-\Sigma(0)} - \frac{1}{p^2}\right], \tag{A1}$$

where $1/p^2$ represents the term with no interaction, $\langle\phi^2\rangle_{u\to 0}$, to be subtracted according to the discussion in Sec. II (compare e.g. with Eq. (1.9)), and

$$\Sigma(p) \equiv \frac{2}{N}\int \frac{d^3\,k}{(2\pi)^3}\;\; F(k)\;\frac{1}{(k+p)^2}\;\;, \tag{A2}$$

with the "dressed" (resummed) scalar propagator (see Fig. 1)

$$F(k) = \left[\frac{6}{N\,u} + B(k)\right]^{-1}\;\;, \tag{A3}$$

where

$$B(k) = \int \frac{d^3\,q}{(2\pi)^3}\;\frac{1}{q^2\;(k+q)^2}\;\;= \frac{1}{8\,k}\,, \tag{A4}$$

represents the basic one-loop (massless) bubble integral. At the relevant (next-to-leading) $1/N$ order one obtains the basic expression to be evaluated as

$$\Delta\langle\phi^2\rangle = -2\;\int \frac{d^3\,p}{(2\pi)^3}\;\frac{d^3\,k}{(2\pi)^3}\;\frac{1}{p^4}\;\left(\frac{6}{N\,u} + B(k)\right)^{-1}\left[\frac{1}{(k+p)^2} - \frac{1}{k^2}\;\right]\;\;, \tag{A5}$$

where the $1/p^2$ subtraction term cancels out with the first order term belonging to the $1/N$ expansion of the term $[p^2 + \Sigma(p) - \Sigma(0)]^{-1}$, in Eq. (A1). Remark that, after applying the HP theorem, all loop integrals in (A5) involve massless scalar propagators. Accordingly, both integrals in Eq. (A5) are IR divergent at intermediate steps, although the final physical result $\Delta\langle\phi^2\rangle$ should be an IR (and UV) convergent quantity. Also, the integral over k is not (absolutely) UV convergent: it has superficially a logarithmic UV divergence. Thus, as emphasized in Refs. [10, 11], one should be very careful to correctly regularize these integrals before doing standard manipulations, like typically exchanging the order of the two integrations in Eq. (A5). The authors of Ref. [10] chose to work in dimensional regularization, which takes care of both, UV and IR divergences. We thus now summarize the main steps of this calculation. First, one integrates over p, so that the second term of the bracket in Eq. (A5) vanishes, since $\int d^d p/p^4 = 0$ in dimensional regularization. The integration of the non-vanishing first term in the bracket of Eq. (A5) gives a result whose behavior for $d \to 3$ is essentially given by $\sim 1/[\Gamma(d-3)]$, that would, naively, give zero as a result. However, it combines with a simple pole in $d-3$ given by the next k integral (see below). More precisely, integration of Eq. (A5) gives (omitting factors that are regular for $d \to 3$):

$$\int \frac{d^d\,p}{(2\pi)^d}\;\frac{1}{p^4\;(k+p)^2} = \frac{1}{(4\pi)^{d/2}}\;\frac{\Gamma(d/2-1)}{\Gamma(d-3)}\;\frac{\pi}{\sin(\pi d/2)}\;k^{d-6}\;\;, \tag{A6}$$

where the space-time dimension d is kept arbitrary, for the moment. One has next to deal with an integral over k of the generic form (omitting again nonessential constant overall factors)

$$I_{\phi^2} \sim \int \frac{d^d\,k}{(2\pi)^d}\;\frac{k^{d-6}}{\frac{6}{N\,u} + B(d)\,k^{d-4}}\;\;, \tag{A7}$$

where $B(d=3) = 1/8$. Next, to evaluate Eq. (A7), we make the following change of variable: $P^2 = k^{-\epsilon}$ where $\epsilon \equiv 4 - d$, which gives

$$d^d k \to \frac{-2}{\epsilon} p^{-d\,(1+2/\epsilon)}\;d^d P\;\;. \tag{A8}$$

Then using the basic dimensional regularization formula:

$$\int \frac{d^d P}{(2\pi)^d}\;\frac{(P^2)^b}{(P^2+R^2)^a} = \frac{1}{(2\pi)^{d/2}}\frac{\Gamma(d/2+b)}{\Gamma(d/2)\,\Gamma(a)}\;\Gamma(a-b-d/2)\;(R^2)^{(d/2+b-a)}\;\;, \tag{A9}$$

we obtain after some algebra

$$I_{\phi^2} \sim \frac{2\pi}{(4\pi)^{d/2}\,(4-d)\,\Gamma(d/2)\sin(2\pi(3-d)/(4-d))}\,B^{2(d-3)/(4-d)}\,\left(\frac{6}{N\,u}\right)^{\frac{2-d}{4-d}}\quad , \tag{A10}$$

where, for $d \to 3$, $\sin^{-1}[2\pi(3-d)/(4-d)]$ combines with $\Gamma^{-1}(d-3)$ to give a finite result[7] proportional to u. Putting back all overall factors, one finds

$$\Delta\langle\phi^2\rangle = -\frac{Nu}{96\pi^2}\quad , \tag{A11}$$

which is simply related to c_1 via Eq. (1.5), in agreement with Ref. [10].

APPENDIX B: LARGE ORDER BEHAVIOR OF STANDARD LDE AND PMS

In this appendix we briefly analyze the large order behavior of the standard LDE, in order to exhibit some generic properties of the LDE-PMS optimization solutions, as well as the link with the more direct CIRT method considered in Sec. IV.B.

Considering either Eq. (3.21) or (3.27) with $\eta^* \equiv \eta(1-\delta)^{1/2}$, the result of its expansion to order k in δ followed by $\delta \to 1$ can be written formally as (the coefficients K_n here refer indistinguishably to either the J_n of Eq. (3.21) or the G_i of Eq. (3.27))

$$\Delta\langle\phi^2\rangle^{(k)}(\eta,u) = -\frac{N\eta}{4\pi}\sum_{n=0}^{k}(-1)^n\frac{\Gamma[3/2]}{n!\,\Gamma[3/2-n]} + \frac{uN}{3}\sum_{n=1}^{k}K_n\left(-\frac{uN}{6\eta}\right)^n\sum_{q=0}^{k-n-1}(-1)^q\frac{\Gamma[1-n/2]}{q!\,\Gamma[1-n/2-q]} \tag{B1}$$

where the last sum originates from the expansion of $(1-\delta)^{-n/2}$ and the upper limit of this sum takes into account that at order k of the δ expansion, there is a term coming from $u(u/\eta)^n \to \delta^{n+1}\,u(u/\eta)^n$ and a term from $(1-\delta)^{-n/2}$. The sums can be performed analytically to give

$$\Delta\langle\phi^2\rangle^{(k)}(\eta,u) = -\frac{N\eta}{4\pi}\sqrt{\pi}\frac{(-1)^k}{\Gamma[1/2-k]\,\Gamma[1+k]} + \frac{uN}{3}\sum_{n=1}^{k}K_n\left(-\frac{uN}{6\eta}\right)^n\frac{\Gamma[-n/2+k]}{\Gamma[-n+k]\,\Gamma[1+n/2]} \tag{B2}$$

The expression (B2) as it stands is particularly convenient to be optimized with respect to η at arbitrary order k, leading to the results shown e.g. in Tables II-VI, X, XI, depending whether one takes the exact $1/N$, IR approximated, or exact $N=2$ values of the relevant perturbative coefficients K_n, given in Eq. (5.2).

The large LDE order behavior, for $k \to \infty$, of expression (B2) can also be analyzed, to give:

$$\Delta\langle\phi^2\rangle^{(k)}(\eta,u) \underset{k\,\to\,\infty}{\sim} -\frac{N\eta}{4\pi}\frac{1}{\sqrt{\pi}\,k^{1/2}} + \frac{uN}{3}\sum_{n=1}^{k}K_n\left(-\frac{uN}{6\eta}\right)^n\frac{k^{n/2}}{\Gamma[1+n/2]}\,, \tag{B3}$$

where we used, to obtain Eq. (B3), the well-known properties of the Gamma functions, such as $\Gamma[2z] = 2^{2z-1/2}\Gamma[z]\,\Gamma[1/2+z]/\sqrt{(}2\pi)$, $\Gamma[z]\,\Gamma[1-z]\sin(\pi z) = \pi$ and the Stirling asymptotic behavior $\Gamma[b+az] \sim \sqrt{2\pi}e^{-az}(az)^{az+b-1/2}$.

Expression (B3) clearly suggests to rescale for convenience the arbitrary mass parameter according to $\eta \to \tilde{\eta}k^{1/2}$. Of course, after such a rescaling the relevant limit is again $\tilde{\eta} \to 0$. After such a rescaling, one obtains

$$\Delta\langle\phi^2\rangle^{(k\to\infty)}(\tilde{\eta},u) \sim -\frac{N\tilde{\eta}}{4\pi}\frac{1}{\Gamma[1/2]} + \frac{uN}{3}\sum_{n=1}^{\infty}\frac{K_n}{\Gamma[1+n/2]}\,\left(-\frac{uN}{6\tilde{\eta}}\right)^n \tag{B4}$$

---

[7] Note a misprint in Eq. (27) of ref.[10], where the relevant term $\sin[2\pi(3-d)/(4-d)]$ reads $\sin[\pi(d-2)/(4-d)]$.

which, as expected, agrees with the CIRT "direct" LDE resummation result Eq. (4.14).
More precisely, for the simpler geometric series cases Eq. (4.2) or Eq. (3.27), corresponding thus to (up to an overall factor) $K_n = 1$, the sum in Eq. (B4) can be further performed exactly, to give: $\exp(x^2)\, Erfc(x) - 1$ with $x \equiv u/\eta$ (or $x \equiv uN/(48\pi\,\eta)$) for Eq. (4.2) (respectively for Eq. (3.27)). Finally the asymptotic expansion of $Erfc(x)$ for the relevant limit $x \to \infty$ (equivalently $\eta \to 0$) [41]:

$$\exp(x^2) Erfc(x) \sim \frac{1}{\sqrt{\pi}\,x}\left[1 + \sum_{q=1}^{\infty}\prod_{i=1}^{q}\left(-\frac{1}{2x^2}\right)^q (2i-1)\right] , \tag{B5}$$

was used at different stages in Sec. IV, for instance to examine the behavior of the LDE series when the linear tadpole term is included in the procedure.

---

[1] N. Goldenfeld, *Lectures on Phase Transitions and The Renormalization Group*, Frontiers in Physics, V. 85 (Addison-Wesley, NY, 1992).
[2] M. Gleiser, R. C. Howell and R. O. Ramos, Phys. Rev. **E65**, 036113 (2002).
[3] K.G. Wilson and J. Kogut, Phys. Rep. **12**, 75 (1974).
[4] J. Zinn-Justin, *Quantum Field Theory and Critical Phenomena* (Oxford University Press, 1996).
[5] Ph. W. Courteille, V. S. Bagnato and V. I. Yukalov, Laser Phys. **11**, 659 (2001); F. Dalfovo, S. Giorgini, L. P. Pitaevskii and S. Stringari, Rev. Mod. Phys. **71**, 463 (1999).
[6] D. G. Barci, E. S. Fraga and R. O. Ramos, Phys. Rev. Lett. **85**, 479 (2000); Laser Phys. **12**, 43 (2002); D. G. Barci, E. S. Fraga, M. Gleiser and R. O. Ramos, Physica **A317**, 535 (2003).
[7] G. Baym, J.-P. Blaizot, M. Holzmann, F. Laloë and D. Vautherin, Phys. Rev. Lett. **83**, 1703 (1999).
[8] P. Arnold, G. Moore and B. Tomásik, Phys.Rev. **A65**, 013606 (2002).
[9] G. Baym, J.-P. Blaizot, M. Holzmann, F. Lalöe and D. Vautherin, arXiv: cond-mat/0107129.
[10] G. Baym, J.-P. Blaizot and J. Zinn-Justin, Europhys. Lett. **49**, 150 (2000).
[11] P. Arnold and B. Tomásik, Phys. Rev. **A62**, 063604 (2000).
[12] A. Okopińska, Phys. Rev. **D35**, 1835 (1987); A. Duncan and M. Moshe, Phys. Lett. **B215**, 352 (1988). See also: H. Kleinert, Fortschr. d. Physik. **30**, 187 (1986); *ibid.* **30**, 351 (1982); and for the strong coupling case: H. Kleinert, Ann. Phys. (N.Y.) **266**, 135 (1998).
[13] V.I. Yukalov, Mosc. Univ. Phys. Bull. **31**, 10 (1976); R. Seznec and J. Zinn-Justin, J. Math. Phys. **20**, 1398 (1979); J.C. LeGuillou and J. Zinn-Justin, Ann. Phys. (N.Y.) **147**, 57 (1983); for a review, see also Chap. 5 in: H. Kleinert, *Path Integrals in Quantum Mechanics, Statistics, Polymer Physics, and Financial Markets* (World Scientific Publishing Co., Singapore, 2001).
[14] P. Arnold and G. Moore, Phys. Rev. Lett. **87**, 120401 (2001); Phys. Rev. **E64**, 066113 (2001).
[15] V.A. Kashurnikov, N.V. Prokof'ev and B.V. Svistunov, Phys. Rev. Lett. **87**, 120402 (2001).
[16] X. Sun, arXiv: hep-lat/0209144.
[17] F. F. de Souza Cruz, M. B. Pinto and R. O. Ramos, Phys. Rev. **B64**, 014515 (2001); Laser Phys. **12**, 203 (2002).
[18] F. F. de Souza Cruz, M. B. Pinto, R. O. Ramos and P. Sena, Phys. Rev. **A65**, 053613 (2002).
[19] D. J. Bedingham and T. S. Evans, Phys. Rev. **D64**, 105018 (2001).
[20] S. Chiku and T. Hatsuda, Phys. Rev. **D58**, 076001 (1998).
[21] M. B. Pinto and R. O. Ramos, Phys. Rev. **D60** , 105005 (1999); *ibid.* **D61** 125016 (2000).
[22] H. F. Jones and P. Parkin, Nucl. Phys. **B594**, 518 (2001).
[23] E. Braaten and E. Radescu, Phys. Rev. Lett. **89**, 271602 (2002); Phys. Rev. **A66**, 063601 (2002).
[24] H. Kleinert, arXiv: cond-mat/0210162.
[25] I.R.C. Buckley, A. Duncan and H.F. Jones, Phys. Rev. **D47**, 2554 (1993); C. M. Bender, A. Duncan and H.F. Jones, Phys. Rev. **D49**, 4219 (1994); C. Arvanitis, H. F. Jones and C.S. Parker, Phys. Rev. **D52**, 3704 (1995).
[26] H. Kleinert and W. Janke, Phys. Lett. **A206**, 283 (1995).
[27] R. Guida, K. Konishi and H. Suzuki, Ann. Phys. (N.Y.) **241** (1995) 152; *ibid.* **249**, 109 (1996).
[28] B. Bellet, P. Garcia and A. Neveu, Int. J. of Mod. Phys. **A11**, 5587 (1997); *ibid.* **A11**, 5607 (1997).
[29] A. Duncan and H. F. Jones, Phys. Rev. **D47**, 2560 (1993).
[30] J.-L. Kneur and D. Reynaud, Eur. Phys. J. **C24**, 323 (2002); Phys. Rev. **D66**, 085020 (2002).
[31] J.-L. Kneur, M. B. Pinto and R. O. Ramos, Phys. Rev. Lett. **89**, 210403 (2002); An *Addendum* to this reference will take into account important quantitative changes and numerical results quoted in the present work.
[32] S. K. Gandhi, H.F. Jones and M. B. Pinto, Nucl. Phys. **B359**, 429 (1991).
[33] G. Krein, D. P. Menezes and M. B. Pinto, Phys. Lett. **B370**, 5 (1996); G. Krein, D. P. Menezes and M.B. Pinto Int. J. of Mod. Phys. **E9**, 221 (2001).
[34] P. M. Stevenson, Phys. Rev. **D23**, 2916 (1981).
[35] C.M. Bender and T.T. Wu, Phys. Rev. 184 (1969) 1231; Phys. Rev. D7 (1973) 1620.
[36] E. Braaten and A. Nieto, Phys. Rev. **D51**, 6990 (1995).

[37] G. P. Lepage, J. Comp. Phys. **27**, 192 (1978).
[38] Mathematica version 3.0, S. Wolfram Company.
[39] For a review on Borel summation method and many original references, see J. C. Le Guillou and J. Zinn-Justin Eds., *Large-Order Behaviour of Perturbation Theory*, Current Physics–Sources and Comments, North-Holland, 1990.
[40] For a review see M. Beneke, Phys. Rep. **317**, 1 (1999).
[41] M. Abramowitz and I.A. Stegun, "*Handbook of Mathematical Functions*" (Dover, N.Y.,1972).
[42] see e.g. G. A Baker, Jr., in *Advances in Theoretical Physics*, Vol. 1, pg. 1 (Academic Press, New York, 1965).
[43] C. Arvanitis, F. Geniet, M. Iacomi, J.-L. Kneur and A. Neveu, Int. J. Mod. Phys. **A12**, 3307 (1997).
[44] B. Kastening, arXiv: cond-mat/0303486.
[45] H. Kleinert, A. Pelster, B. Kastening and M. Bachmann, Phys. Rev **E62**, 1537 (2000); hep-th/0105193; H. Kleinert and V. Schulte-Frohlinde, *Critical Properties of* ϕ^4 *Theories* (World Scientific, Singapore, 2001); http://www.physik.fu-berlin.de∼kleinert/294/programs.

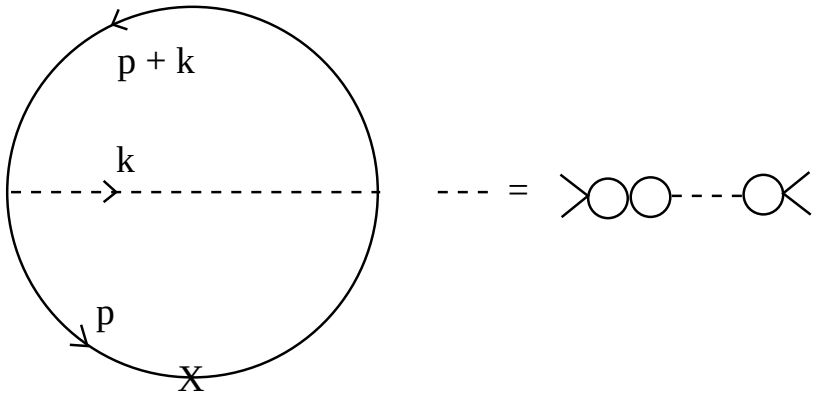

FIG. 1: The Feynman graph for the relevant quantity $\langle\phi^2\rangle_u$ at $1/N$ order, with the resummed propagator (dotted lines).

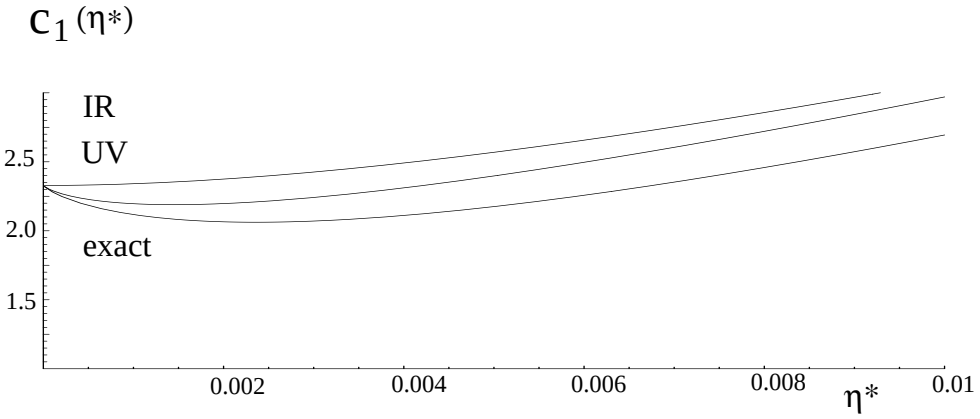

FIG. 2: Comparison between the naive IR, UV propagator approximation Eq. (3.25), (3.26), and the exact numerical integration of Eq. (3.16), before subtracting the spurious contribution $Nu/(96\pi^2)$.

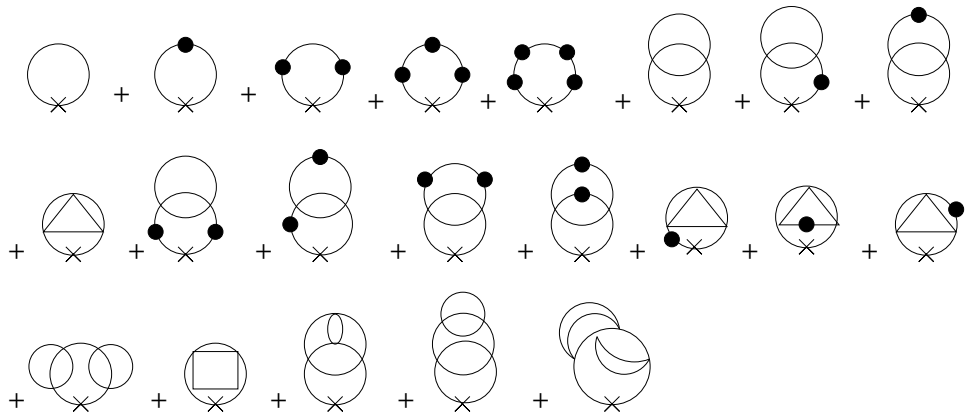

FIG. 3: All diagrams contributing to $\langle\phi^2\rangle_u^{(4)}$ at the critical point. The black dot represents the $\delta\eta^2$ insertions.

TABLE I: LDE of the simple alternated geometric series, Eq.(4.1). PMS optimization results, at different LDE orders k.

k	$S0$	$S1$	$S2$	$S3$	$S4$	$S5$
1	$\sqrt{2}$	$-\sqrt{2}$	–	–	–	–
2	1.69743	-1.12996	–	–	–	–
	–	$\pm 0.167336I$	–	–	–	–
3	1.81088	-1.00296	-1.11978	–	–	–
	–	$\pm 0.129109I$	–	–	–	–
4	1.87082	-0.959082	-1.06361	–	–	–
	–	$\pm 0.076116I$	$\pm 0.0465028I$	–	–	–
5	1.90768	-0.950095	-1.02417	-1.05508	–	–
	–	$\pm 0.03648I$	$\pm 0.0499I$	–	–	–
6	1.93258	-0.954501	-1.00183	-1.03612	–	–
	–	$\pm 0.01086I$	$\pm 0.0407I$	$\pm 0.019I$	–	–
7	1.95052	-0.9630	-0.99069	-1.01992	-1.03154	–
	–	$\pm 0.00447I$	$\pm 0.02932I$	$\pm 0.02416I$		–
8	1.96405	-0.9719	-0.9861	-1.0085	-1.02313	–
	–	$\pm 0.01304I$	$\pm 0.01929I$	$\pm 0.023I$	$\pm 0.0096I$	–
9	1.97462	-0.9797	-0.9851	-1.0012	-1.01516	-1.0205
	–	$\pm 0.0174I$	$\pm 0.0114I$	$\pm 0.0195I$	$\pm 0.01346I$	–
10	1.9831	-0.9861	-0.9859	-0.9968	-1.0088	-1.016
	–	$\pm 0.019I$	$\pm 0.0056I$	$\pm 0.0154I$	$\pm 0.0141I$	± 0.0055

TABLE II: Standard LDE at large-N, Eq. (3.21). PMS results for c_1, at different orders k, obtained with all families.

k	$F0$	$F1$	$F2$	$F3$	$F4$	$F5$	$F6$	$F7$	$F8$	$F9$	$F10$
2	-2.163	2.163	–	–	–	–	–	–	–	–	–
3	-2.698	1.879	–	–	–	–	–	–	–	–	–
	–	$\pm 0.169I$	–	–	–	–	–	–	–	–	–
4	-2.945	1.713	1.962	–	–	–	–	–	–	–	–
	–	$\pm 0.061I$	–	–	–	–	–	–	–	–	–
5	-3.087	1.642	1.913	–	–	–	–	–	–	–	–
	–	$\pm 0.077I$	$\pm 0.029I$	–	–	–	–	–	–	–	–
6	-3.179	1.620	1.870	1.935	–	–	–	–	–	–	–
	–	$\pm 0.196I$	$\pm 0.008I$	–	–	–	–	–	–	–	–
7	-3.244	1.622	1.843	1.928	–	–	–	–	–	–	–
	–	$\pm 0.293I$	$\pm 0.067I$	$\pm 0.001I$	–	–	–	–	–	–	–
8	-3.292	1.636	1.829	1.921	1.935	–	–	–	–	–	–
	–	$\pm 0.369I$	$\pm 0.128I$	$\pm 0.025I$	–	–	–	–	–	–	–
9	-3.329	1.654	1.825	1.913	1.936	1.946	–	–	–	–	–
	–	$\pm 0.429I$	$\pm 0.184I$	$\pm 0.062I$	–	–	–	–	–	–	–
10	-3.358	1.675	1.828	1.908	1.938	1.950	–	–	–	–	–
	–	$\pm 0.476I$	$\pm 0.233I$	$\pm 0.102I$	–	$\pm 0.027I$	–	–	–	–	–
11	-3.382	1.696	1.836	1.907	1.940	1.950	1.966	–	–	–	–
	–	$\pm 0.515I$	$\pm 0.276I$	$\pm 0.139I$	–	$0.056I$	–	–	–	–	–
12	-3.402	1.715	1.845	1.909	1.941	1.950	1.972	–	–	–	–
	–	$\pm 0.546I$	$\pm 0.313I$	$\pm 0.174I$	–	$\pm 0.086I$	$\pm 0.025I$	–	–	–	–
13	-3.419	1.733	1.856	1.913	1.942	1.950	1.974	1.983	–	–	–
	–	$\pm 0.571I$	$\pm 0.344I$	$\pm 0.206I$	–	$\pm 0.114I$	$0.050I$	–	–	–	–
14	-3.433	1.750	1.868	1.919	1.942	1.952	1.976	1.988	–	–	–
	–	$\pm 0.592I$	$\pm 0.372I$	$\pm 0.234I$	–	$\pm 0.141I$	$\pm 0.075I$	$\pm 0.023I$	–	–	–
15	-3.445	1.765	1.880	1.926	1.943	1.956	1.978	1.992	1.997	–	–
	–	$\pm 0.610I$	$\pm 0.395I$	$\pm 0.260I$	–	$\pm 0.166I$	$\pm 0.098I$	$\pm 0.045I$	–	–	–
16	-3.456	1.780	1.891	1.934	1.944	1.960	1.981	1.995	2.002	–	–
	–	$\pm 0.625I$	$\pm 0.416I$	$\pm 0.282I$	–	$\pm 0.189I$	$\pm 0.119I$	$\pm 0.066I$	$\pm 0.021I$	–	–
17	-3.466	1.792	1.903	1.942	1.944	1.966	1.984	1.998	2.006	2.010	–
	–	$\pm 0.638I$	$\pm 0.433I$	$\pm 0.302I$	–	$\pm 0.210I$	$\pm 0.140I$	$\pm 0.085I$	$\pm 0.040I$	–	–
18	-3.474	1.804	1.913	1.950	1.945	1.972	1.988	2.000	2.009	2.014	–
	–	$\pm 0.649I$	$\pm 0.449I$	$\pm 0.321I$	–	$\pm 0.229I$	$\pm 0.159I$	$\pm 0.104I$	$\pm 0.059I$	$\pm 0.019I$	–
19	-3.482	1.815	1.924	1.959	1.945	1.978	1.992	2.004	2.012	2.018	2.020
	–	$\pm 0.658I$	$\pm 0.463I$	$\pm 0.337I$	–	$\pm 0.246I$	$\pm 0.177I$	$\pm 0.121I$	$\pm 0.076I$	$\pm 0.036I$	–
20	-3.488	1.825	1.933	1.967	1.945	1.984	1.997	2.007	2.016	2.021	2.025
	–	$\pm 0.666I$	$\pm 0.475I$	$\pm 0.351I$	–	$\pm 0.262I$	$\pm 0.193I$	$\pm 0.138I$	$\pm 0.092I$	$\pm 0.053I$	$\pm 0.017I$

TABLE III: Standard LDE at large-N, Eq.(3.21). Three families of PMS and Fastest Apparent Convergence (FAC) results for c_1.

k	$F1-PMS$	$F1-FAC$	$F2-PMS$	$F2-FAC$	$F3-PMS$	$F3-FAC$
2	2.163	2.498	–	–	–	–
3	$1.879 \pm 0.169I$	$1.884 \pm 0.274I$	–	–	–	–
4	$1.713 \pm 0.061I$	$1.660 \pm 0.097I$	1.962	1.996	–	–
5	$1.642 \pm 0.077I$	$1.593 \pm 0.078I$	$1.913 \pm 0.029I$	$1.917 \pm 0.0462I$	–	–
6	$1.620 \pm 0.196I$	$1.585 \pm 0.213I$	$1.870 \pm 0.008I$	$1.858 \pm 0.003I$	1.935	1.941
7	$1.622 \pm 0.293I$	$1.600 \pm 0.314I$	$1.843 \pm 0.067I$	$1.826 \pm 0.063I$	$1.928 \pm 0.001I$	$1.928 \pm 0.005I$
8	$1.636 \pm 0.369I$	$1.622 \pm 0.390I$	$1.829 \pm 0.128I$	$1.813 \pm 0.130I$	$1.921 \pm 0.025I$	$1.915 \pm 0.0213I$
9	$1.654 \pm 0.429I$	$1.647 \pm 0.448I$	$1.825 \pm 0.184I$	$1.811 \pm 0.189I$	$1.913 \pm 0.062I$	$1.905 \pm 0.061I$
10	$1.675 \pm 0.476I$	$1.671 \pm 0.493I$	$1.828 \pm 0.233I$	$1.817 \pm 0.241I$	$1.908 \pm 0.102I$	$1.899 \pm 0.102I$
11	$1.696 \pm 0.514I$	$1.694 \pm 0.529I$	$1.836 \pm 0.276I$	$1.827 \pm 0.284I$	$1.907 \pm 0.139I$	$1.898 \pm 0.141I$
12	$1.715 \pm 0.545I$	$1.715 \pm 0.558I$	$1.845 \pm 0.313I$	$1.839 \pm 0.321I$	$1.908 \pm 0.174I$	$1.901 \pm 0.178I$
13	$1.733 \pm 0.571I$	$1.734 \pm 0.582I$	$1.856 \pm 0.344I$	$1.852 \pm 0.353I$	$1.913 \pm 0.206I$	$1.906 \pm 0.210I$
14	$1.750 \pm 0.592I$	$1.752 \pm 0.601I$	$1.868 \pm 0.371I$	$1.865 \pm 0.380I$	$1.919 \pm 0.234I$	$1.913 \pm 0.239I$
15	$1.765 \pm 0.610I$	$1.767 \pm 0.618I$	$1.880 \pm 0.395I$	$1.877 \pm 0.403I$	$1.926 \pm 0.260I$	$1.921 \pm 0.265I$
16	$1.780 \pm 0.625I$	$1.782 \pm 0.631I$	$1.891 \pm 0.416I$	$1.890 \pm 0.423I$	$1.934 \pm 0.282I$	$1.930 \pm 0.287I$
17	$1.792 \pm 0.638I$	$1.795 \pm 0.643I$	$1.903 \pm 0.433I$	$1.902 \pm 0.440I$	$1.942 \pm 0.302I$	$1.939 \pm 0.308I$
18	$1.804 \pm 0.649I$	$1.807 \pm 0.654I$	$1.913 \pm 0.449I$	$1.913 \pm 0.455I$	$1.950 \pm 0.321I$	$1.947 \pm 0.326I$
19	$1.815 \pm 0.658I$	$1.817 \pm 0.663I$	$1.924 \pm 0.463I$	$1.923 \pm 0.468I$	$1.959 \pm 0.337I$	$1.957 \pm 0.342I$
20	$1.825 \pm 0.666I$	$1.827 \pm 0.670I$	$1.933 \pm 0.475I$	$1.934 \pm 0.480I$	$1.967 \pm 0.351I$	$1.966 \pm 0.356I$

TABLE IV: Infrared LDE at large-N, Eq.(3.27). PMS results for c_1, at different orders k.

k	$F0$	$F1$	$F2$	$F3$	$F4$	$F5$	$F6$	$F7$	$F8$	$F9$	$F10$
2	-2.852	2.852	–	–	–	–	–	–	–	–	–
3	-3.577	2.444	–	–	–	–	–	–	–	–	–
	–	$\pm 0.276I$	–	–	–	–	–	–	–	–	–
4	-3.910	2.244	2.482	–	–	–	–	–	–	–	–
	–	$\pm 0.200I$	–	–	–	–	–	–	–	–	–
5	-4.100	2.184	2.397	–	–	–	–	–	–	–	–
	–	$\pm 0.097I$	$\pm 0.079I$	–	–	–	–	–	–	–	–
6	-4.223	2.184	2.333	2.397	–	–	–	–	–	–	–
	–	$\pm 0.020I$	$\pm 0.081I$	–	–	–	–	–	–	–	–
7	-4.309	2.205	2.298	2.369	–	–	–	–	–	–	–
	–	$\pm 0.028I$	$\pm 0.060I$	$\pm 0.032I$	–	–	–	–	–	–	–
8	-4.372	2.232	2.283	2.342	2.366	–	–	–	–	–	–
	–	$\pm 0.055I$	$\pm 0.037I$	$0.040I$	–	–	–	–	–	–	–
9	-4.214	2.256	2.279	2.324	2.354	–	–	–	–	–	–
	–	$\pm 0.068I$	$\pm 0.016I$	$\pm 0.036I$	$\pm 0.016I$	–	–	–	–	–	–
10	-4.460	2.277	2.282	2.313	2.341	2.352	–	–	–	–	–
	–	$\pm 0.074I$	$\pm 0.010I$	$\pm 0.028I$	$\pm 0.022I$	–	–	–	–	–	–
11	-4.498	2.294	2.287	2.307	2.331	2.346	–	–	–	–	–
	–	$\pm 0.074I$	$\pm 0.010I$	$\pm 0.019I$	$\pm 0.022I$	$0.009I$	–	–	–	–	–
12	-4.518	2.307	2.293	2.305	2.324	2.339	2.345	–	–	–	–
	–	$\pm 0.072I$	$\pm 0.017I$	$\pm 0.011I$	$\pm 0.019I$	$0.014I$	–	–	–	–	–
13	-4.540	2.317	2.299	2.305	2.319	2.333	2.341	–	–	–	–
	–	$\pm 0.068I$	$\pm 0.022I$	$\pm 0.004I$	$\pm 0.015I$	$0.015I$	$\pm 0.006I$	–	–	–	–
14	-4.559	2.324	2.305	2.306	2.316	2.328	2.337	2.340	–	–	–
	–	$\pm 0.064I$	$\pm 0.025I$	$\pm 0.001I$	$\pm 0.011I$	$0.014I$	$\pm 0.009I$	–	–	–	–
15	-4.575	2.330	2.310	2.308	2.315	2.324	2.333	2.338	–	–	
	–	$\pm 0.061I$	$\pm 0.027I$	$\pm 0.005I$	$\pm 0.007I$	$0.012I$	$\pm 0.010I$	$\pm 0.004I$	–	–	–
16	-4.589	2.334	2.315	2.310	2.314	2.322	2.330	2.335	2.338	–	–
	–	$\pm 0.057I$	$\pm 0.027I$	$\pm 0.008I$	$\pm 0.004I$	$0.010I$	$\pm 0.010I$	$\pm 0.006I$	–	–	–
17	-4.602	2.338	2.318	2.313	2.314	2.320	2.327	2.333	2.336	–	–
	–	$\pm 0.053I$	$\pm 0.027I$	$\pm 0.010I$	$\pm 0.001I$	$0.008I$	$\pm 0.009I$	$\pm 0.007I$	$\pm 0.003I$	–	–
18	-4.613	2.340	2.322	2.315	2.315	2.319	2.325	2.330	2.334	2.336	–
	–	$\pm 0.050I$	$\pm 0.027I$	$\pm 0.012I$	$\pm 0.001I$	$0.005I$	$\pm 0.008I$	$\pm 0.007I$	$\pm 0.004I$	–	–
19	-4.623	2.342	2.324	2.317	2.316	2.319	2.324	2.329	2.332	2.335	–
	–	$\pm 0.047I$	$\pm 0.026I$	$\pm 0.013I$	$\pm 0.003I$	$0.003I$	$\pm 0.007I$	$\pm 0.007I$	$\pm 0.005I$	$\pm 0.002I$	–
20	-4.631	2.344	2.327	2.319	2.317	2.319	2.323	2.327	2.331	2.333	2.334
	–	$\pm 0.045I$	$\pm 0.025I$	$\pm 0.014I$	$\pm 0.005I$	$0.002I$	$\pm 0.005I$	$\pm 0.006I$	$\pm 0.007I$	$\pm 0.003I$	–

TABLE V: Comparison of Infrared and exact LDE at large-N, for $\eta = R_c^{-1} = 1/(24\pi)$ at different orders k.

k	1	2	3	4	5	6	7	8	9	10	
IR	1.16424	3.20165	1.89188	2.67411	2.17385	2.47173	2.27958	2.39236	2.31806	2.36035	
exact	1.16424	2.2129	1.78534	1.98289	1.892	1.94579	1.92615	1.94536	1.94367	1.95312	
k	11	12	13	14	15	16	17	18	19	20	100
IR	2.33129	2.34685	2.33524	2.34073	2.33590	2.33765	2.33549	2.33588	2.33481	2.33474	2.32910
exact	1.95614	1.9624	1.96651	1.9715	1.97566	1.97999	1.98393	1.98782	1.99149	1.99504	2.10987

TABLE VI: Best PMS results for c_1, at different orders k, from the exact LDE series at large-N when omitting the tadpole term $-(N\eta)/(4\pi)$.

k	3	4	5	6	10	15
c_1	1.061	$1.222 \pm 0.37I$	1.34	$1.435 \pm 0.720I$	$1.710 \pm 0.99I$	$1.896 \pm 1.089I$
k	20	30	50	60	80	100
c_1	$1.999 \pm 1.120I$	$2.129 \pm 0.880I$	$2.243 \pm 0.900I$	$2.272 \pm 0.910I$	$2.311 \pm 0.780I$	$2.33 \pm 0.69I$

TABLE VII: Standard LDE at large-N, Eq. (4.14). All CIRT-PMS results for c_1, at different orders k.

k	$F0$	$F1$	$F2$	$F3$	$F4$	$F5$	$F6$	$F7$	$F8$	$F9$	$F10$
2	-2.818	2.818	–	–	–	–	–	–	–	–	–
3	-3.400	2.000	–	–	–	–	–	–	–	–	–
	–	$\pm 0.814I$	–	–	–	–	–	–	–	–	–
4	-3.554	1.219	2.428	–	–	–	–	–	–	–	–
	–	$\pm 0.669I$	–	–	–	–	–	–	–	–	–
5	-3.597	0.750	2.121	–	–	–	–	–	–	–	–
	–	$\pm 0.242I$	$\pm 0.408I$	–	–	–	–	–	–	–	–
6	-3.610	0.506	1.734	2.246	–	–	–	–	–	–	–
	–	$\pm 0.247I$	$\pm 0.463I$	–	–	–	–	–	–	–	–
7	-3.613	0.416	1.422	2.096	–	–	–	–	–	–	–
	–	$\pm 0.740I$	$\pm 0.336I$	$\pm 0.233I$	–	–	–	–	–	–	–
8	-3.614	0.448	1.205	1.882	2.147	–	–	–	–	–	–
	–	$\pm 1.228I$	$\pm 0.127I$	$\pm 0.304I$	–	–	–	–	–	–	–
9	-3.614	0.587	1.071	1.681	2.062	–	–	–	–	–	–
	–	$\pm 1.691I$	$\pm 0.115I$	$\pm 0.269I$	$\pm 0.146I$	–	–	–	–	–	–
10	-3.614	0.836	1.001	1.518	1.932	2.087	–	–	–	–	–
	–	$\pm 2.138I$	$\pm 0.365I$	$\pm 0.171I$	$\pm 0.206I$	–	–	–	–	–	–
11	-3.614	1.203	0.998	1.397	1.797	2.034	–	–	–	–	–
	–	$\pm 2.552I$	$\pm 0.609I$	$\pm 0.038I$	$\pm 0.200I$	$\pm 0.097I$	–	–	–	–	–
12	-3.614	1.701	1.040	1.317	1.678	1.949	2.047	–	–	–	–
	–	$\pm 2.913I$	$\pm 0.841I$	$\pm 0.111I$	$\pm 0.151I$	$\pm 0.143I$	–	–	–	–	–
13	-3.614	2.343	1.126	1.272	1.581	1.856	2.012	–	–	–	–
	–	$\pm 3.190I$	$\pm 1.054I$	$\pm 0.266I$	$\pm 0.073I$	$\pm 0.148I$	$\pm 0.067I$	–	–	–	–
14	-3.614	3.142	1.251	1.58	1.506	1.768	1.954	2.020	–	–	–
	–	$\pm 3.339I$	$\pm 1.243I$	$\pm 0.419I$	$\pm 0.021I$	$\pm 0.122I$	$\pm 0.102I$	–	–	–	–
15	-3.614	4.106	1.412	1.272	1.455	1.691	1.887	1.996	–	–	–
	–	$\pm 3.301I$	$\pm 1.401I$	$\pm 0.566I$	$\pm 0.125I$	$\pm 0.073I$	$\pm 0.110I$	± 0.048	–	–	–
16	-3.614	5.229	1.606	1.309	1.424	1.628	1.821	1.955	2.001	–	–
	–	$\pm 2.996I$	$\pm 1.525I$	$\pm 0.702I$	$\pm 0.232I$	$\pm 0.010I$	$\pm 0.095I$	± 0.074	–	–	–
17	-3.614	6.491	1.828	1.367	1.411	1.579	1.761	1.906	1.984	–	–
	–	$\pm 2.327I$	$\pm 1.604I$	$\pm 0.825I$	$\pm 0.339I$	$\pm 0.062I$	$\pm 0.063I$	± 0.082	$\pm 0.035I$	–	–
18	-3.614	7.838	2.071	1.442	1.416	1.544	1.709	1.855	1.954	1.988	–
	–	$\pm 1.169I$	$\pm 1.632I$	$\pm 0.932I$	$\pm 0.442I$	$\pm 0.140I$	$\pm 0.019I$	± 0.073	$\pm 0.055I$	–	–
19	-3.614	9.181	2.327	1.532	1.434	1.522	1.665	1.807	1.917	1.975	–
	–	$\pm 0.628I$	$\pm 1.600I$	$\pm 1.022I$	$\pm 0.539I$	$\pm 0.220I$	$\pm 0.033I$	± 0.051	$\pm 0.061I$	$\pm 0.025I$	–
20	-3.614	10.360	2.584	1.634	1.466	1.513	1.632	1.764	1.877	1.952	1.978
	–	$\pm 3.236I$	$\pm 1.499I$	$\pm 1.091I$	$\pm 0.628I$	$\pm 0.299I$	$\pm 0.091I$	± 0.019	$\pm 0.055I$	$\pm 0.041I$	–

TABLE VIII: Infrared LDE at large-N, Eq. (4.15). All CIRT-PMS large-N results for c_1, at different orders k.

k	$F1$	$F2$	$F3$	$F4$	$F5$	$F6$	$F7$	$F8$	$F9$
2	2.328	–	–	–	–	–	–	–	–
3	2.328	2.262	2.395	–	–	–	–	–	–
4	2.328	2.320	2.337	–	–	–	–	–	–
	–	$\pm 0.067I$	$\pm 0.067I$	–	–	–	–	–	–
5	2.328	2.369	2.287	2.271	2.386	–	–	–	–
	–	$\pm 0.054I$	$\pm 0.054I$	–	–	–	–	–	–
6	2.328	2.389	2.268	2.294	2.363	–	–	–	–
	–	$\pm 0.027I$	$\pm 0.027I$	$\pm 0.041I$	$\pm 0.041I$	–	–	–	–
7	2.328	2.391	2.266	2.323	2.334	2.281	2.376	–	–
	–	$\pm 0.005I$	$\pm 0.005I$	$\pm 0.050I$	$\pm 0.050I$	–	–	–	–
8	2.328	2.386	2.270	2.344	2.313	2.293	2.364	–	–
	–	$\pm 0.011I$	$0.011I$	$\pm 0.045I$	$\pm 0.045I$	$\pm 0.025I$	$\pm 0.025I$	–	–
9	2.328	2.379	2.278	2.357	2.300	2.310	2.347	2.289	2.368
	–	$\pm 0.021I$	$\pm 0.021I$	$\pm 0.036I$	$\pm 0.036I$	$\pm 0.036I$	$\pm 0.036I$	–	–
10	2.328	2.371	2.286	2.363	2.294	2.325	2.332	2.296	2.360
	–	$\pm 0.027I$	$\pm 0.027I$	$\pm 0.025I$	$\pm 0.025I$	$\pm 0.038I$	$\pm 0.038I$	$\pm 0.017I$	$\pm 0.017I$

TABLE IX: PMS optimization of Padé approximants (based both on the original and CIRT improved series for two of the relevant families) for c_1 in the large N case with the exact series coefficients.

k	$P[1,2]$ PMS		$P[1,2]$ CIRT		$P[0,3]$ PMS		$P[0,3]$ CIRT	
3	2.623	2.034	2.01 ± 0.14 I	–	2.328 ± 0.18 I	–	2.328 ± 0.05I	–
4	2.61	2.05	1.877 ± 0.34 I	2.02	2.328 ± 0.17 I	–	2.328 ± 0.05I	–
5	2.615 ± 0.10 I	2.04 ± 0.1 I	1.77 ± 0.61 I	1.98 ± 0.06 I	2.29 ± 0.2 I	2.37 ± 0.19 I	2.34 ± 0.05I	2.33 ± 0.05 I

TABLE X: All ordinary PMS and CIRT-improved PMS optimization for c_1 in the finite $N = 2$ case.

k	$F0$ PMS	$F0$ CIRT	$F1$ PMS	$F1$ CIRT	$F2$ PMS	$F2$ CIRT
2	-3.05916	-3.98590	3.05916	3.98590	–	–
3	-4.47035	- 5.97078	2.44730	3.10543	–	–
	–	–	$\pm 1.65256I$	$\pm 3.09300I$	–	–
4	-5.30592	-7.03900	1.53443	1.19134	3.14286	5.22847
	–	–	$\pm 2.29581I$	$\pm 4.33683I$	–	–

TABLE XI: Same as previous table for c_1 in the finite $N = 2$ case, but with IR large N perturbative coefficient K_i for $i > 3$

k	$F0$ PMS	$F0$ CIRT	$F1$ PMS	$F1$ CIRT	$F2$ PMS	$F2$ CIRT
2	-3.059	-3.986	3.059	3.986	–	–
3	-4.470	- 5.971	2.447	3.105	–	–
	–	–	$\pm 1.653I$	$\pm 3.093I$	–	–
4	-5.306	-7.039	1.534	1.194	3.143	5.106
	–	–	$\pm 2.296I$	$\pm 4.337I$	–	–
5	-5.717	-7.05	1.352	1.176	3.71	5.09
	–	–	$\pm 2.83I$	$\pm 4.33I$	–	–
6	-5.97	-7.05	1.29	1.179	4.00	5.09
	–	–	$\pm 3.13I$	$\pm 4.32I$	–	–
10	-6.43	-7.05	1.219	1.179	4.49	5.09
	–	–	$\pm 3.66I$	$\pm 4.32I$	–	–

TABLE XII: PMS optimization of Padé approximants (based both on the original and CIRT improved series for two of the relevant families) for finite $N = 2$ case.

k	$P[1,2]$ PMS		$P[1,2]$ CIRT		$P[0,3]$ PMS		$P[0,3]$ CIRT	
3	2.62	2.04	2.01 ± 0.20 I	–	2.328 ± 3.24 I	–	1.37	3.28
4	2.60	2.06	1.98 ± 0.41 I	1.98	2.328 ± 3.07 I	–	0.97 ± 0.34 I	3.15
5	2.63 ± 0.07 I	2.02 ± 0.07 I	1.97 ± 0.62 I	1.94 ± 0.12 I	1.51 ± 3.45 I	3.15 ± 3.45 I	1.11 ± 0.44 I	3.17
10	2.60 ± 0.04 I	2.05 ± 0.04 I	1.82 ± 0.31 I	1.88 ± 0.11 I	1.20 ± 1.65 I	3.45 ± 1.65 I	1.15 ± 0.11 I	3.27